The Chemistry of Metallic Elements in the Ionosphere and Mesosphere

THEODORE L. BROWN

Materials Research Laboratory and School of Chemical Sciences, University of Illinois, Urbana, Illinois 61801, and International Meteorological Institute, Stockholm, Sweden

Received March 9, 1973 (Revised Manuscript Received May 31, 1973)

Contents

I. Introduction

This review is concerned mainly with the chemical behavior of metallic elements in the upper atmosphere, in the altitude interval from about 50 to 120 km. Before the chemical processes which determine the chemical states of the metals can be understood, however, one must have an appreciation for the aeronomic considerations involved. The radiation flux, atmospheric temperature, and concentrations of species with which reaction might occur vary with altitude, time of day, season, and location. Transport processes also play an important role in affecting the vertical distributions of metallic species. We begin, therefore, with a brief review of the aeronomic features of principal importance. For a more detailed and balanced introduction to aeronomy the reader is referred to the excellent text by Whitten and Poppoff.[1]

The second major portion of the review concerns the experimental data relating to the presence of metals in the mesophere and above, hypotheses regarding origin, and some considerations regarding transport.

The chemical behavior of the metals is reviewed in detail in the third major section. Although the chemistry of the ionospheric metals has been considered by several others, there has heretofore been no attempt to set out a complete chemical "map" which takes into account the altitude and diurnal variations of the important atmospheric constituents, and which takes account over the entire altitude range of interest of all the reactions which might be of importance. This review therefore is an attempt to put forth such a complete chemical description. On the basis of it, one can assess the probable degree to which the metallic elements are in chemical equilibrium at any given altitude, and for different times of day. The calculated altitude profiles of the metallic species of interest, and various other quantities derivable from the chemical model presented, are compared with experimental results in a final section.

II. The Atmosphere

A. Temperature, Number Density

The temperature profile of the atmosphere, as given by the 1965 CIRA COSPAR International Reference Atmosphere,[2] is shown in Figure 1. The region of immediate interest extends from about 120 km to the stratopause, in the vicinity of 50 km. The temperature minimum at the mesopause varies with latitude and time of year. It becomes as low as 130°K in summer at high latitudes.[3-5]

Table I lists the number densities of molecular nitrogen and oxygen, and of atomic oxygen as a function of elevation, for the 1965 COSPAR reference atmosphere. The total number density is that obtained for the temperature profile shown in Figure 1. The actual number densities and temperature profiles exhibit diurnal and seasonal variations. The reference atmosphere represents mean values based on extensive observational data.

In discussing the variation in number density (*i.e.*, pressure) with altitude, it is common to speak in terms of *scale height*, the distance in which the number density of the atmosphere as a whole, or of some particular component, decreases by a factor $1/e$. In an isothermal atmosphere of constant composition, the scale height of total pressure is a constant, given by $kT/\bar{m}g$: $\bar{m}$ is the mean molecular weight and g is the gravitational acceleration.

B. Radiation, Ionization Processes

As solar radiation enters the earth's atmosphere, it is absorbed by various atmospheric constituents. Some of

(1) R. C. Whitten and I. C. Poppoff, "Fundamentals of Aeronomy," Wiley, New York, N. Y., 1971.

(2) "CIRA 1965, COSPAR International Reference Atmosphere 1965," North-Holland Publishing Co., Amsterdam, 1965.

(3) G. Witt, J. Martin-Löf, N. Wilhelm, and W. S. Smith, *Space Res.*, **5**, 820 (1965).

(4) J. S. Theon, N. Nordberg, and W. S. Smith, *Science*, **157**, 419 (1967).

(5) J. S. Theon, W. Nordberg, L. B. Katchen, and J. J. Horvath, *J. Atmos. Sci.*, **24**, 428 (1967).

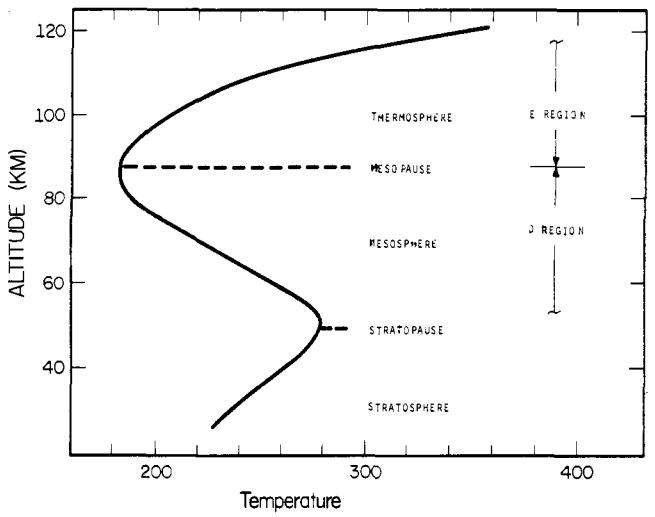

Figure 1. Temperature profile of the CIRA 1965, COSPAR reference atmosphere.[2]

TABLE I. O_2, N_2 and O Number Densities at Various Altitudes[a]

Altitude, km	N_2, cm^{-3}	O_2, cm^{-3}	O, cm^{-3}	T, °K
70	1.34(15)	3.59(14)	...	217
75	6.74(14)	1.74	...	201
80	2.96	7.95(13)	8.5(10)	186
85	1.21	3.25	9.8	186
90	4.96(13)	1.33	1.25(11)	186
95	1.95	5.19(12)	3.4	198
100	8.18(12)	1.99	5.0	208
105	3.45	7.93(11)	3.6	229
110	1.62	3.49	2.0	251
115	7.46(11)	1.50	1.24	303
120	4.00	7.50(10)	7.6(10)	355

[a] The convention employed in this review will be to write a number such as 1.34×10^{15} as 1.34(15). Data from CIRA COSPAR 1965 Reference Atmosphere.[2]

this absorption results in production of ions. The major ion productions are shown in Figure 2.[6,7]

Absorption of short-wavelength radiation by O_2 and N_2 in the upper atmosphere is extensive, so that there is little flux of extreme uv and uv solar radiation below 100 km. An exception to this generalization is the hydrogen Lyman α line at 121.6 nm, for which there remains a high flux below 100 km. The only atmospheric component of significant abundance in the vicinity of the mesopause with a sufficiently low ionization potential to undergo ionization from H Lyman α radiation is NO. Production of NO^+ is therefore the major ion production process near 80 km. Above the NO^+ region, O_2^+ and N_2^+ productions dominate.

Galactic cosmic radiation contributes relatively little to ionization in the daytime atmosphere above 70 km. Since the optical depth is very large, the importance of this ultrahigh energy as ionization source increases in proportion to the number density. All atmospheric components display comparable cross-sections toward cosmic ray ionization.

In the night sky the major source of ionization is, of course, shut off, and ionization sources of otherwise secondary importance then make significant contributions to the chemical activity. For example, a nightglow H Lyman

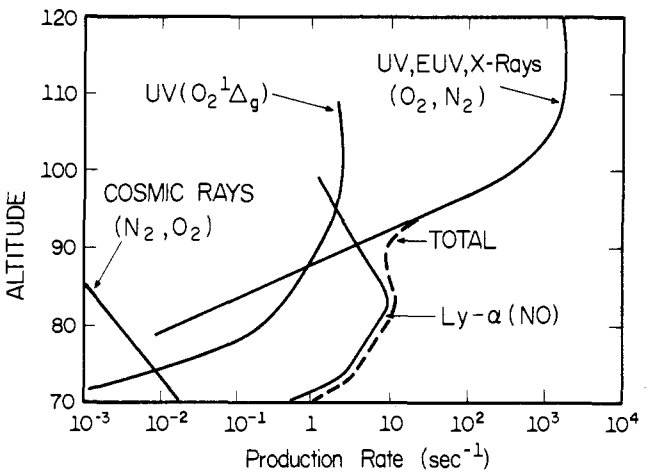

Figure 2. Ion production rates in the upper atmosphere. The production rates resulting from solar radiation correspond to a solar zenith angle $\chi = 58°$. The figure is after Reid,[6] except that the ionization rate for $O_2(^1\Delta_g)$ has been adjusted downward as calculated by Huffman, *et al.*[7]

β radiation (102.6 mm) originating in the hydrogen geocorona and transported radiatively to the dark side of the hemisphere is believed responsible for a persistent nighttime ionization of O_2 in the E region.[8-10] NO is thought to be ionized by scattered H Lyman α radiation.[10]

In addition to the radiant sources of ionization which dominate the ionization processes under normal or undisturbed conditions, other irregular sources may at various times dominate, particularly in the polar latitudes. During a polar cap absorption (PCA) event, ionization is due mainly to energetic protons.[11] Production rates of O_2^+ and N_2^+ below 85 km are increased appreciably over undisturbed conditions in even a moderately intense proton shower.[12] Energetic electrons are also frequently "precipitated" in the polar auroral zone.[11,13] Impact of high-energy (40 keV) electrons on atmospheric molecules results in production of X-rays, whereas electrons with energies of 10 keV or less produce predominantly direct excitation and/or ionization. Electrons with energy 40 keV or less do not penetrate significantly below about 90 km.

For a given atmospheric composition and set of radiation conditions, the production rates of various ion species are determined. The steady-state concentrations of the ions are in turn determined by the rates of chemical processes such as charge exchange and dissociative recombination, *e.g.*[14]

$$N_2^+ + O_2 \rightarrow N_2 + O_2^+ \ (4.7 \times 10^{-11}) \quad (1)$$

$$O_2^+ + NO \rightarrow NO^+ + O_2 \ (8 \times 10^{-10}) \quad (2)$$

$$O + N_2^+ \rightarrow NO^+ + N \ (2.5 \times 10^{-10}) \quad (3)$$

$$O_2^+ + e^- \rightarrow O + O \ (2.1 \times 10^{-7}) \quad (4)$$

(6) G. C. Reid, *J. Geophys. Res.*, **75**, 2551 (1970).
(7) R. E. Huffman, D. E. Paulsen, and J. C. Larrabee, *J. Geophys. Res.*, **76**, 1028 (1971).
(8) W. Swider, *J. Geophys. Res.*, **70**, 4859 (1965).
(9) J. M. Young, G. R. Carruthers, J. C. Holmes, C. Y. Johnson, and N. P. Patterson, *Science*, **160**, 990 (1968).
(10) T. Ogawa and T. Tohmatsu, *Rep. Ionos. Space Res. Jap.*, **20**, 395 (1966).
(11) B. M. McCormac, Ed., "The Radiating Atmosphere," D. Reidel Publishing Co., Dordrecht, Holland, 1972.
(12) G. C. Reid in "Magnetosphere-Ionosphere Interactions," K. Folkestad, Ed., Norwegian Universities Press, Oslo, 1972.
(13) T. A. Poterma and A. J. Zmuda, *J. Geophys. Res.*, **75**, 7161 (1970).
(14) E. W. McDaniel, V. Cermak, A. Dalgarno, E. E. Ferguson, and L. Friedman, "Ion-Molecule Reactions," Wiley-Interscience, New York, N. Y., 1970, Table 6-1, pp 321-332.

TABLE II. Photoionization Rates for Atomic Metals, for Unattenuated Solar Flux[22]

Metal	Photoionization rate, sec^{-1}	Metal	Photoionization rate, sec^{-1}
Li	2.7×10^{-4}	Ca	3.5×10^{-5}
Na	1.7×10^{-5}	Si	1.5×10^{-5}
K	2.9×10^{-5}	Fe	5×10^{-7}
Mg	4×10^{-7}	Ni	1.5×10^{-6}

where rate constants in units of cm^3 sec^{-1} at 300°K are given in parentheses. Thus, although N_2^+ is copiously produced in the altitude range 100–160 km, it is not a major ionic component because of rapid reactions such as (1) and (3).

The number of possible reactions is very large (*vide infra*), and values for many of the important rate constants are not known. These uncertainties, coupled with great variability in the sources of ionization preclude precise modelling of the ionosphere. Nevertheless, substantial progress has been made in identifying the important reaction sequences. Thus, for example, the presence of hydronium hydrates $H(H_2O)_n^+$ in the mesosphere, established by several rocket investigations,[15] can be accounted for to a fair degree using reaction schemes based largely on rate constants measured in laboratory experiments.[16-20]

C. Photoionization of Metallic Species

The neutral metallic species which are likely to be the most important candidates for ionization are the metal atoms and monoxides. The photoionization rate is a product of the photoionization cross-section and the solar flux, integrated from the short wavelength side to the ionizing wavelength limit. The photoionization cross-sections for the elements helium to xenon have been calculated by McGuire.[21] Use of these values and the unattenuated solar flux gives upper limits to the photoionization rates.

Swider[22] has made approximate calculations of the photoionization rates for some metals using data from several sources (Table II). Calculations of this type are not very accurate because the results are sensitive to the resolution in the cross-section and flux data and to the size of the step in the integration process. Further, to more realistically reflect the solar flux below 120 km, the tabulated values should probably be reduced somewhat. The results are sufficiently reliable to suggest, however, that photoionization of many metals is not likely to be important in comparison with other ion production processes (to be described later) in the 120–80-km range.

Cross-section data for molecular metal-containing species are essentially nonexistent. The monoxides should exhibit an ionization potential at least as large, and probably larger, than that for the free metal. As a very rough guide, one might assume that the monoxides closely parallel the free metal atoms in photoionization behavior and, accordingly, that photoionization can be disregarded as compared with other ionization processes. As will become evident later, the neutral metal oxides are not important above 90 km.

D. Electrons and Negative Ions

Production of molecular ions by photoionization as in eq 5-7 leads to free electrons. In the absence of loss

$$N_2 + h\nu \rightarrow N_2^+ + e^- \quad (5)$$

$$O_2 + h\nu \rightarrow O_2^+ + e^- \quad (6)$$

$$NO + h\nu \rightarrow NO^+ + e^- \quad (7)$$

processes other than recombination with one of the positive ions, the free electron population should equal the total positive ion population. Furthermore, assuming that large regions of excess net charge density do not develop, the electron and total positive ion profiles should correspond closely. This is probably the case down to about 75 km during undisturbed conditions, but at lower elevation negative ions appear. These arise *via* attachment of electrons to O_2 in a three-body reaction

$$O_2 + e^- + M \rightarrow O_2^- + M \quad (8)$$

The O_2^- ion, once formed, undergoes charge-transfer reaction with a neutral component of the atmosphere, neutralization by reaction with a positive ion, or photodetachment of the electron. Laboratory studies of negative ion processes[23-27] reveal that many reactions are likely to occur rapidly in the mesosphere, leading to a high degree of complexity in the negative ion composition. The reaction sequences beginning with O_2^- lead to negative ions such as NO_3^-, CO_3^-, or CO_4^-,[6,28] For our purposes, the most important consideration is the *total* negative ion density, because the only reaction likely to be of importance between negative ions and the metallic species is neutralization, e.*g.*

$$M^+ + O_2^- \rightarrow M + O_2 \quad (9)$$

$$MO^+ + NO_3^- \rightarrow MO + NO_3 \quad (10)$$

Neutralization may be expected to have about the same rate constant for all negative ions. The variation of total negative ion population with altitude is therefore more important than the relative abundances of the various negative ions.

The concentration profiles for free electrons above 80 km are fairly well known for many conditions and from the results of independent methods of measurement. Figures 3 and 4 show experimental electron density profiles.[29,30] The negative ion profiles, by contrast, are not well established. Narcisi and coworkers[31] found fairly heavy concentrations of negative ions with masses from 12 to 162 amu in the altitude range 73–90 km, in a nighttime rocket experiment launched from the Fort Churchill, Canada, range. Arnold, Krankowsky, and coworkers, on the other hand, found a moderately sharp cut-off of negative ions above about 78 km in a nighttime experiment launched from Andoya, Norway.[32]

(15) R. S. Narcisi and W. Roth, *Advan. Electron. Electron Phys.*, **29**, 79 (1970).
(16) A. Good, D. A. Durden, and P. Kebarle, *J. Chem. Phys.*, **52**, 222 (1970).
(17) E. E. Ferguson and F. C. Fehsenfeld, *J. Geophys. Res.*, **74**, 5743 (1969).
(18) F. C. Fehsenfeld, M. Mosesman, and E. E. Ferguson, *J. Chem. Phys.*, **55**, 2115 (1971).
(19) J. M. Heimerl, J. A. Vanderhoff, L. J. Puckett, G. E. Keller, and F. E. Niles, U. S. Army Ballistics Research Laboratories, Report No. 1605, 1972.
(20) F. E. Niles, J. M. Heimerl, G. E. Keller, and L. J. Puckett, *Radio Sci.*, **7**, 117 (1972).
(21) E. J. McGuire, *Phys. Rev.*, **175**, 20 (1968).
(22) W. Swider, Jr., *Planet. Space Sci.*, **17**, 1233 (1969).
(23) F. C. Fehsenfeld and E. E. Ferguson, *Planet. Space Sci.*, **16**, 701 (1968).
(24) A. V. Phelps, *Can. J. Chem.*, **47**, 1783 (1969).
(25) L. Pack and A. V. Phelps, *Bull. Amer. Phys. Soc.*, 16, 214 (1971).
(26) E. E. Ferguson, *Ann. Geophys.*, **26**, 589 (1970).
(27) R. P. Turco and C. F. Sechrist, Jr., *Radio Sci.*, **7**, 725 (1972).
(28) F. Arnold and D. Krankowsky, *J. Atmos. Terr. Phys.*, **33**, 1693 (1971).
(29) C. F. Sechrist, Jr., *J. Atmos. Terr. Phys.*, **30**, 371 (1968).
(30) E. A. Mechtly and L. G. Smith, *J. Atmos. Terr. Phys.*, **30**, 1555 (1968).
(31) R. S. Narcisi, A. D. Bailey, L. Della Lucca, C. Sherman, and D. M. Thomas, *J. Atmos. Terr. Phys.*, **33**, 1147 (1971).

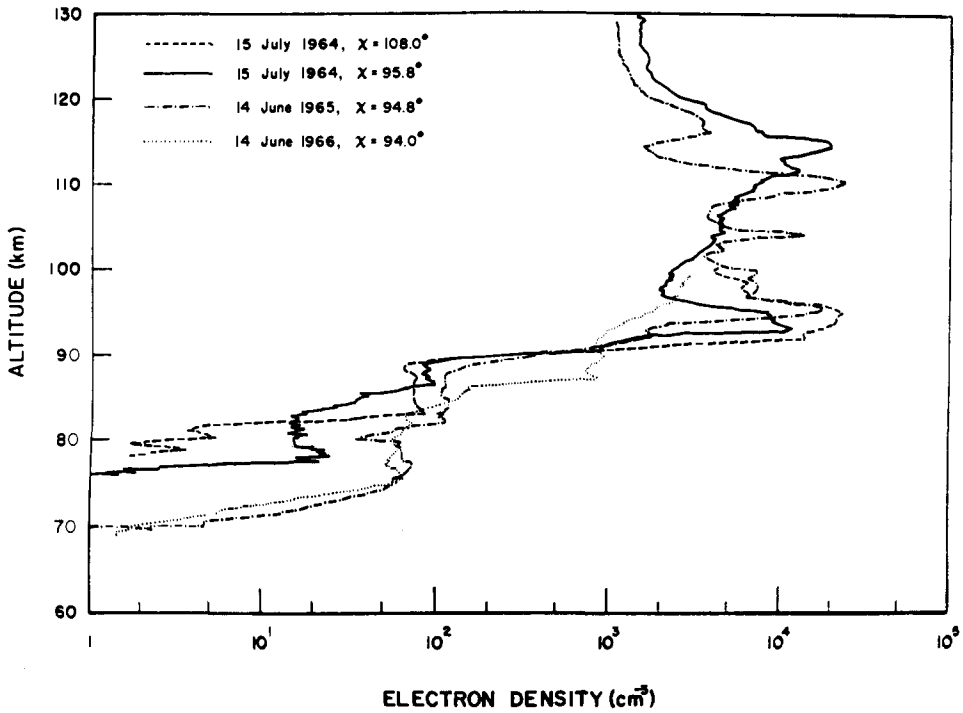

Figure 3. Electron density profiles at various sunrise and presunrise times, Wallops Island, Va.[29]

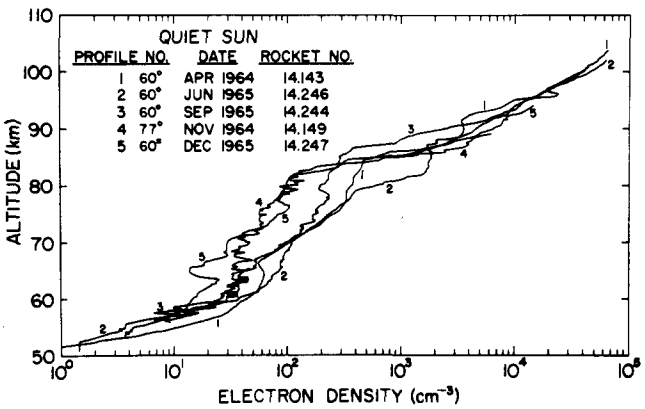

Figure 4. A seasonal comparison of five daytime electron density profiles taken during the International Quiet Sun Year.[30]

Although electron concentrations have been measured at altitudes well below 60 km and upward, experimental difficulties have so far prevented quantitative evaluations of the negative ion levels. Indeed, even crude estimates of relative abundances are attained only above about 75 km. Thus, all that can be said by way of general remarks is that in the nighttime the negative charge should exist below 80 km in the form of negative ions. In the daytime, photodetachment reactions should occur, leading to relatively higher ratio of free electrons to negative ions. Even so, negative ions probably dominate below 70 km.

III. Chemical Reactions of Ionic Species

A. Production

Production of ionic species occurs principally *via* photoionization as already described. It is possible, however, for chemi-ionization to occur, e.g.

$$CH + O \rightarrow CHO^+ + e^- \qquad (11)$$

Although this particular reaction has been invoked[33] as a significant contributor to ionization in the D region, there is as yet no firm evidence[34] that it or any other chemi-ionization process is in fact important there.

TABLE III. Cross-Sections for Ionizing Collisions between Neutral Species[35]

Metal atom	Speed, km/sec	$\sigma(10^{-16}$ cm^2) O_2	$\sigma(10^{-16}$ cm^2) N_2
Fe	80	0.8	0.25
	100	1.3	0.4
Si	120	0.7	0.5
	143	1	0.85
Mg	125	0.2	0.2
	154	0.3	0.3
Ca	65	0.3	0.25
	98	0.85	0.5

Collisions between atoms and/or small molecules at high energies could lead to ionization. This could be particularly important for metal atoms ablating from meteoroids which enter the atmosphere at very high speeds. The cross-sections for a few processes of this type have been measured (Table III).[35] Consideration of these and other results suggests that ionization by collision is relatively unimportant as compared with thermalization of the atoms *via* kinetic energy transfer.[36-38]

Ionization may occur *via* charge-transfer processes of the type shown in Table IV. Tabulated rates for other reactions of this type are to be found in ref 14 and 39. These reactions are exothermic when the ionization potential of the neutral molecule is less than the electron affinity of the ion. Because of its relatively low ionization

(32) F. Arnold, J. Kissel, D. Krankowsky, H. Wieder, and J. Zähringer, *J. Atmos. Terr. Phys.*, **33**, 1161 (1971).
(33) R. R. Burke, *J. Geophys. Res.*, 77, 1998 (1972).
(34) W. Swider, *J. Geophys. Res.*, 77, 2000 (1972).
(35) A. M. Bukhteev and Y. D. Bydin, *Izv. Akad. Nauk SSSR*, **27**, 1009 (1963); *Bull. Acad. Sci. USSR, Phys. Ser.*, **27**, 985 (1963).
(36) F. Verniani, *Space Sci. Rev.*, **10**, 230 (1969).
(37) D. W. Sida, *Mon. Notices, Roy. Astron. Soc.*, **143**, 37 (1969).
(38) M. Gadsden, *Ann. Geophys.*, **25**, 721 (1969).
(39) F. Kaufman, *Ann. Rev. Phys. Chem.*, **20**, 45 (1969).
(40) P. D. Goldan, A. L. Schmeltekopf, F. C. Fehsenfeld, H. I. Schiff, and E. E. Ferguson, *J. Chem. Phys.*, **44**, 4095 (1966).
(41) J. A. Rutherford, R. F. Mathis, B. R. Turner, and D. A. Vroom, *J. Chem. Phys.*, **56**, 4654 (1972).

TABLE IV. Charge-Transfer Ionization Processes at 300°K

Reaction	k, cm³ sec⁻¹	Ref
$N_2^+ + NO \rightarrow N_2 + NO^+$	5.0(−10)	40
$O_2^+ + NO \rightarrow O_2 + NO^+$	8.0(−10)	40
$O_2^+(X^2\Pi_g) + Na \rightarrow O_2 + Na^+$	13.8(−10)	41
$N_2^+ + Na \rightarrow N_2 + Na^+$	18.9(−10)	41
$NO^- + Mg \rightarrow NO + Mg^-$	8.1(−10)	42, 43
$N_2^+ + Mg \rightarrow N_2 + Mg^+$	7.2(−10)	42, 43
$O_2^+(X^2\Pi_g) + Mg \rightarrow O_2 + Mg^+$	12.3(−10)	42, 43
$NO^- + Na \rightarrow NO + Na^+$	$\sim 10^{-10}$	41
$N_2^+ + H_2O \rightarrow N_2 + H_2O^+$	2.2(−9)	44

potential, 9.27 eV,[45] NO behaves as a positive charge sink with respect to most other atmospheric components. The metals of aeronomic importance in the mesosphere and above, however, possess still lower ionization potentials (Fe, 7.90 eV; Mg, 7.64 eV; Na, 5.14 eV; Ca, 6.11 eV; Si, 8.15 eV).

The excess energy of a charge-transfer reaction may appear as vibrational excitation in the diatomic product molecule or—where the energy is sufficient—could lead to dissociation. In addition, the metal ion may be formed in an excited state. These reactions appear to occur predominantly *via* simple electron transfer. Paulson and coworkers,[46,47] using ^{18}O labeling, showed, for example, that the process

$$^{18}O^+ + NO \rightarrow NO^+ + {}^{18}O \quad (12)$$

predominates over alternative pathways

$$^{18}O^+ + NO \rightarrow N{}^{18}O^+ + O \quad (13)$$

$$\rightarrow {}^{18}OO^+ + N \quad (14)$$

Charge-transfer reactions do not exhibit pronounced temperature dependence. The reactions involving Na show a slight decrease in rate as temperature is increased to 600 and 900°K. The reactions with Mg show a very small increase with increasing temperature. It is noteworthy that charge-transfer reactions involving electron transfer to triatomic molecule-ions are considerably faster than those involving electron transfer to diatomic or atomic ions.

Equations 15–17 show examples of a reaction type commonly classified as charge transfer but, in fact, distinctly different in a chemical sense; in that charge transfer occurs in the course of chemical bond formation and rupture.

$$NO(H_2O)_3^+ + H_2O \rightarrow H_3O(H_2O)_2^+ + HONO \quad (15)$$
$$k = 7 \times 10^{-11}\ cm^3\ sec^{-1},\ 296°K^{48-50}$$

$$O_2(H_2O)^+ + H_2O \xrightarrow{k_a} H_3O(OH)^+ O_2 \quad (16)$$
$$\xrightarrow{k_b} H_3O^+ + OH + O_2$$
$$k_a = 1.9 \times 10^{-9}\ cm^3\ sec^{-1},\ 295°K^{18}$$
$$k_b < 3 \times 10^{-10}\ cm^3\ sec^{-1},\ 295°K^{18}$$

$$Ca(H_2O)^+ + H_2O \rightarrow CaOH^+ + H_3O^+ \quad (17)$$
$$k = 5 \times 10^{-11}\ cm^3\ sec^{-1},\ 300°K^{51}$$

(42) J. A. Rutherford, R. F. Mathis, B. R. Turner, and D. A. Vroom, *J. Chem. Phys.*, **55**, 3785 (1971).

(43) A. L. Farragher, J. A. Peden, and W. L. Fite, *J. Chem. Phys.*, **50**, 287 (1969).

(44) C. J. Howard, H. W. Rundle, and F. Kaufman, *J. Chem. Phys.*, **53**, 3745 (1970).

(45) D. W. Turner and D. P. May, *J. Chem. Phys.*, **45**, 471 (1966).

(46) J. F. Paulson, Record of the Third Aeronomy Conference, University of Illinois-Urbana, Aeronomy Report No. 32, C. F. Sechrist, Ed., Aeronomy Laboratory, University of Illinois-Urbana, 1969 (Final Report, Contract USDAA-005-69-C-0002, Ballistics Research Laboratories, Aberdeen Proving Ground, Md.).

(47) J. F. Paulson, *Recent Develop. Mass Spectrosc., Proc. Int. Conf. Mass. Spectrosc., 1969*, 935 (1970).

TABLE V. Rates of Ion-Molecule (Clustering) Reactions at about 300°K

Reaction	k, cm³ sec⁻¹	Ref
$NO^+ + CO + CO \rightarrow NO(CO)^+ + CO$	2(−30)	52
$NO^+ + CO_2 + CO_2 \rightarrow NO(CO_2)^+ + CO_2$	2(−29)	52
$NO^+ + H_2O + N_2 \rightarrow NO(H_2O)^+ + N_2$	1.4–1.6(−28)	48–50
$NO(H_2O)^+ + H_2O + N_2 \rightarrow NO(H_2O)_2^+ + N_2$	1.0–1.2(−27)	48–50
$NO(H_2O)_2^+ + H_2O + N_2 \rightarrow NO(H_2O)_3^+ + N_2$	1.4–2.0(−27)	48–50
$N_2^+ + N_2 + N_2 \rightarrow N_2(N_2)^+ + N_2$	8(−29)	53
$O_2^+ + O_2 + O_2 \rightarrow O_2(O_2)^+ + O_2$	2.4(−30)	18
$O_2^- + H_2O + O_2 \rightarrow O_2(H_2O)^+ + O_2$	1.9(−28)	18
$Mg^+ + O_2 + Ar \rightarrow MgO_2^+ + Ar$	2(−30)	54
$Ca^+ + O_2 + Ar \rightarrow CaO_2^+ + Ar$	7(−30)	54
$Ca^+ + O_2 + He \rightarrow CaO_2^+ + He$	2(−30)	51
$Fe^+ + O_2 + Ar \rightarrow FeO_2^+ + Ar$	1(−30)	54
$Na^+ + O_2 + Ar \rightarrow NaO_2^+ + Ar$	<2(−31)[a]	54
$K^+ + O_2 + Ar \rightarrow KO_2^+ + Ar$	<2(−31)[a]	54
$Na^+ + H_2O + H_2O \rightarrow Na(H_2O)^+ + H_2O$	1(−28)	55
$Na^+ + H_2O + He \rightarrow Na(H_2O)^+ + He$	4.7(−30)	55
$K^+ + H_2O + H_2O \rightarrow K(H_2O)^+ + H_2O$	4.5(−29)	55
$K^+ + H_2O + He \rightarrow K(H_2O)^+ + He$	2.6(−30)	55
$H_3O^+ + H_2O + N_2 \rightarrow H_3O(H_2O)^+ + N_2$	3(−27)	53
$H_3O(H_2O)^+ + H_2O + N_2 \rightarrow H_3O(H_2O)_2^+ + N_2$	2(−27)	53
$H_3O(H_2O)_2^+ + H_2O + N_2 \rightarrow H_3O(H_2O)_3^+ + N_2$	2(−27)	53

[a] No reaction observed.

B. Clustering

Atomic and molecular ions may, upon collision with neutral species, form ion-neutral complexes. These so-called ion-molecule reactions are a common phenomenon in mass spectrometry and have been the subject of extensive study. Several examples of aeronomic interest, often referred to as clustering reactions, are listed in Table V. More extensive tables are to be found in ref 14 and 39.

Understanding of such reactions has increased immensely during the past few years as detailed kinetic and thermodynamic studies have been carried forward in several laboratories. The clustering reaction is a three-body process of the general form

$$X^+ + A + M \rightarrow XA^+ + M \quad (18)$$

where M may be any molecule or atom. In general, there is ordinarily not much difference in the third-body efficiencies of Ar, N_2, or O_2.

For a given third-body M, the rates of the clustering reactions vary over several orders of magnitude. In an exothermic ion-molecule reaction X^+ and A may be thought to form an intermediate, sometimes referred to as an orbiting complex, which through collision with M is then deactivated with respect to dissociation.[56-58] The

(48) L. J. Puckett and M. W. Teague, *J. Chem. Phys.*, **54**, 2564 (1971).

(49) C. J. Howard, H. W. Rundle, and F. Kaufman, *J. Chem. Phys.*, **55**, 4772 (1971).

(50) F. C. Fehsenfeld, M. Mosesman, and E. E. Ferguson, *J. Chem. Phys.*, **55**, 2120 (1971).

(51) K. G. Spears and F. C. Fehsenfeld, *J. Chem. Phys.*, **56**, 5698 (1972).

(52) J. M. Heimerl and J. A. Vanderhoff, *Bull. Amer. Phys. Soc.*, 17 (II), 392 (1972).

(53) A. Good, D. A. Durden, and P. Kebarle, *J. Chem. Phys.*, **52**, 212 (1972).

(54) E. E. Ferguson and F. C. Fehsenfeld, *J. Geophys. Res.*, **73**, 6215 (1968).

(55) R. Johnsen, H. L. Brown, and M. A. Biondi, *J. Chem. Phys.*, **55**, 186 (1971).

(56) D. K. Bohme, D. B. Dunkin, F. C. Fehsenfeld, and E. E. Ferguson, *J. Chem. Phys.*, **51**, 863 (1969).

(57) D. K. Bohme, *Can. J. Chem.*, **47**, 1809 (1969).

(58) A. Good, *Trans. Faraday Soc.*, **67**, 3495 (1971).

TABLE VI. Rates of Recombination Reactions of Molecular Ions

	k, cm^3 sec^{-1}	Ref
$O_2^+ + e^- \rightarrow O + O$	2.1(−7)	63
$N_2^+ + e^- \rightarrow N + N$	2.5(−7)	63
$NO^+ + e^- \rightarrow N + O$	4.1(−7)	63
$O_2O_2^+ + e^- \rightarrow O_2 + O_2$	1(−6)	64
$H_3O^+ + e^- \rightarrow H + H_2O$	1.1(−6)	65
$H_3O(H_2O)^+ + e^- \rightarrow H + 2H_2O$	2.4(−6)	65
$H_3O(H_2O)_2^+ + e^- \rightarrow H + 3H_2O$	4.7(−6)	65
$H_3O(H_2O)_6^+ + e^- \rightarrow H + 6H_2O$	1.0(−5)	65

cross-section for formation of the complex is related to the electrostatic interaction between X^+ and A. The effective lifetime of the orbiting complex is longer at lower relative kinetic energies and higher reduced mass for the (X^+-A) couple. In general, the rates of three-body ion–molecule reactions are greatest when A is polar or polarizable.[59] The reactions exhibit an apparently negative Arrhenius energy, assuming a temperature dependence of the form

$$k = Ae^{-E_a/kT} \tag{19}$$

The temperature dependence, however, is not large, and it is usually not possible to distinguish between an exponential temperature dependence and one of the form $k = A(E_a/RT)$.[39] As a rough rule, the rate constant at 200°K, a temperature generally characteristic of the region about the mesopause, should be about twice that at 300°K, where the rates are most commonly measured.

Ion–molecule clusters, once formed, may undergo rapid switching reactions, typified by the following.

$$O_2 \cdot O_2^+ + H_2O \rightarrow O_2 \cdot H_2O^+ + O_2 \tag{20}$$

$k = 1.3\text{-}2.2 \times 10^{-9}$ cm^3 sec^{-1}, ~300°K[16,18,60]

$$NO \cdot NO^+ + H_2O \rightarrow NO \cdot H_2O^+ + NO \tag{21}$$

$k = 1.4 \times 10^{-9}$ cm^3 sec^{-1}, 296°K[48]

C. Recombination

Atomic and molecular ions may recombine with electrons to form neutral species.[61] In the case of atoms the energy of recombination is released by emission of a photon.

$$A^+ + e^- \rightarrow A + h\nu \tag{22}$$

The rates of radiative recombination have been calculated for several atomic species.[62] In general, they are quite small, on the order of 1×10^{-12} sec^{-1}.

For the simpler molecular ions, dissociative recombination[61] (eq 23) prevails over possible three-body processes as given by eq 24. The rates of several dissociative recombination reactions are given in Table VI. Although the data are quite limited, it does appear that the rates increase over a range of almost two orders of magnitude for the more complex molecular ions, as exemplified by the higher hydronium hydrates, as compared with the simple diatomic molecular ions.

$$AX^+ + e^- \rightarrow A + X \tag{23}$$

$$AX^+ + e^- + M \rightarrow AX + M^* \tag{24}$$

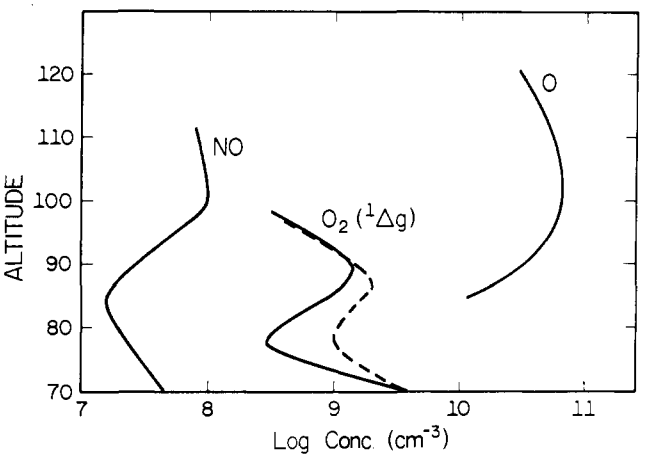

Figure 5. Experimentally determined concentration profiles of a few minor neutral atmosphere constituents. The NO profile is due to Meira.[69] The O profile is based on mass spectral data from the Aladdin experiment.[70] The $O_2(^1\Delta_g)$ profiles (−, morning twilight, $\chi = 90°$; ---, evening twilight, $\chi = 90°$) are due to Wood.[71]

D. Neutralization

Since the ionization potentials of negative ions are generally lower than the electron affinity of positive ions, neutralization reactions are universally exothermic for the simple species observed in the upper atmosphere. Thorough fundamental studies of simple neutralization reactions have been carried out, particularly with the aim of elucidating the relative importances of electron transfer in a bimolecular step and three-body processes.[66,67] For the number densities of interest here, a direct electron-transfer process should prevail. As an example of the considerations involved, the rate of the reaction

$$N^+ + O^- \rightarrow N + O \tag{25}$$

has been studied as a function of relative energies of the two ions.[68] The rate constant increases from a limiting value of 9×10^{-8} cm^3 sec^{-1} at relative energies of 0.5 eV and higher to 1.4×10^{-7} at relative energy of 0.1 eV. It will be assumed in a later section that all relevant neutralization reactions employed in describing the chemistry of the metals possess a rate constant of 1×10^{-7} cm^3 sec^{-1}.

III. The Neutral Atmosphere

A. Distribution of Neutral Minor Constituents

Absorption of solar energy leads also to photodissociation in addition to the photoionization already discussed. The concentrations of "minor" atmospheric constituents which prevail under a given set of radiation conditions, for a particular temperature and number density, are determined by a complex set of interrelated reactions. Unfortunately, it is extremely difficult to obtain reliable experimental profiles of elusive but nevertheless very important minor constituents such as O_3, O, NO, and H in the altitude range 120–70 km. Figure 5 shows a few recently determined profiles.

(59) G. E. Keller and F. E. Niles, *Chem. Phys. Lett.*, **10**, 526 (1971).
(60) C. J. Howard, V. M. Bierbaum, H. W. Rundle, and F. Kaufman, *J. Chem. Phys.*, **57**, 3491 (1972).
(61) D. R. Bates, *Contemp. Phys.*, 11, 105 (1970).
(62) D. R. Bates and A. Dalgarno, "Atomic and Molecular Processes," D. R. Bates, Ed., Academic Press, New York, N. Y., 1962, p 245.
(63) J. N. Beardsley and M. A. Biondi, *Advan. At. Mol. Phys.*, **6**, 1 (1970).
(64) W. H. Kasner and M. A. Biondi, *Phys. Rev.*, **174**, 139 (1968).
(65) M. T. Leu, M. A. Biondi, and R. Johnsen, *Phys. Rev. A*, **7**, 292 (1973).
(66) B. H. Mahan and J. C. Person, *J. Chem. Phys.*, **40**, 392 (1964).
(67) B. H. Mahan, *Advan. Chem. Phys.*, **23**, 1 (1973).
(68) W. Aberth, J. R. Peterson, D. C. Lorrents, and C. J. Cook, *Phys. Rev. Lett.*, **20**, 979 (1968).

TABLE VII.[a] Calculated Concentrations of Species of Interest in the Neutral Atmosphere[72,73]

Alt, km	O_3		O		O_2	H
	A	B	A	B		
110	1.4(5)	7.8(5)	2.8(11)	2.6(11)	2.4(11)	3.6(6)
105	1.3(6)	3.7(6)	4.7	4.5	6.5	8.4
100	8.5	1.3(7)	6.2	6.0	1.8(12)	2.0(7)
95	5.7(7)	5.9(7)	9.0	8.8	5.2	5.4
90	1.1(8)	1.0(8)	4.9	4.6	1.4(13)	1.4(8)
85	6.9(7)	4.4(7)	9.1(10)	5.7(10)	3.8	2.9
80	2.1(8)	7.8(6)	2.6	...	9.6	1.8
75	4.5(8)	3.1(8)	4.1(9)	...	2.1(14)	6.0(7)
70	4.9(9)	5.1(9)	2.5(9)	...	4.2	7.0(6)
65	1.0(10)	1.0(10)	...	...	8.2(14)	

[a] The A columns refer to evening twilight conditions and the B columns to morning twilight. There is essentially no variation in the concentrations of O_2 and H for these two times. (The O_2 profile differs from that listed in Table I because a slightly different temperature profile was assumed in the calculations.)

The comparative values are of little significance because in general the separate experimental studies have not been carried out under the same conditions with respect to season, time of day, latitude, or the prevalence of disturbances. Furthermore, the absolute calibrations of the profiles in terms of number density are difficult. The desired profile is often not very directly related to the experimental observable, but must be inferred from the data with the aid of several assumptions. For example, the NO profile has been deduced from a photometric experiment in which the NO γ-band emissions at 214.9 and 204.7 nm were observed from a rocket in the twilight sky.[69] The emission observed is that from a column of atmosphere at some angle with respect to the zenith. This angle changes with rocket rotation and nutation as the vehicle moves vertically. The contribution of NO to the observed emission must be deduced after correcting for atmospheric Raleigh scattering and correcting for the rocket's motion. It is then a further step to deduce the local concentration of NO at a particular altitude from the observed variation in the emission as a function of rocket elevation.

Rocket-borne mass spectral determinations of the local concentrations of neutral species are in principle more immediately relatable to the local concentration of a given constituent.[70] There are difficulties, however, in correcting for shock-wave effects resulting from the rocket's supersonic velocity and in calibrating the ionization source and detector. In addition, the sensitivity of the method is not high enough for measuring the less abundant minor constituents.

Because of experimental difficulties, there are no experimental results regarding the levels of certain important minor atmospheric constituents, e.g., water vapor above 30 km. The only acceptable data for NO are those of Meira.[69] In view of the importance of this molecule in ionospheric chemistry, it is highly desirable that NO profiles be determined by independent methods, for various atmospheric conditions and latitudes.

The increased availability of spectroscopic data and laboratory-based measurements of reaction rates has made it possible in recent years to develop model atmospheres. Such model systems are usually applicable to a particular altitude range, in which a particular set of chemical processes serves to adequately define the chemistry. Using such a model, and with the aid of simplifying assumptions regarding diffusion processes, it is possible to calculate the prevailing concentrations of all the minor atmospheric constituents for a given set of conditions. A set of such results for a model atmosphere, which includes vertical transport[72,73] in the form of a vertical wind, is given in Table VII. Comparison of these results with those recently reported by Hunt[74] reveals agreement to within an order of magnitude in the 70–120-km interval. Several less abundant species included in the model, e.g., O_2H and H_2O_2, are omitted from the tabulation.

TABLE VIII. Representative Reactions and Rate Constants of Neutral Species[a]

Reaction	Rate constant
$N + O_3 \rightarrow NO + O_2$	$\sim 1\ (-13)$
$NO + O_3 \rightarrow NO_2 + O_2$	$\sim 3\ (-14)$
$O + O_3 \rightarrow 2O_2$	$7.5(-15)\ (298°)$[b]
$O + O_2 + Ar \rightarrow O_3 + Ar$	$4(-34)$
$O + NO + Ar \rightarrow NO_2 + Ar$	$7(-32)$
$Cl + NO + Ar \rightarrow ClNO + Ar$	$8(-32)$
$O + O + N_2 \rightarrow O_2 + N_2$	$3(-33)$
$N + O + N_2 \rightarrow NO + N_2$	$1(-32)$

[a] The second-order rate constants for the first two reactions (in cm^3/sec) are summaries of data listed by K. Schofield, *Planet. Space Sci.*, **15**, 643 (1967), from several sources. Similarly the third-order rates constants are summarized from data listed by Kaufman.[39] The third-body efficiencies of Ar, N_2, and O_2 are within a factor of 2 of being the same in all of the three-body reactions listed for which the relevant data are available. [b] J. L. McCrumb and F. Kaufman, *J. Chem. Phys.*, **57**, 1270 (1972). $k = (1.05 \pm 0.18)10^{-11} \exp(-4.3 \times 10^3/RT)$.

B. Chemical Reactions of Neutral Species

In describing the chemistry of the metals, we will be concerned with several types of reactions of neutral species. The ionization of neutral species to form ions, through photoionization or charge exchange, has already been considered (section III.A). Unfortunately, very little else is known of the kinetics of reaction of neutral metal atoms. Reactions with O_2 to form MO + O may be discounted, because the reaction is endothermic for all the metals of interest except possibly Fe. Reaction with $O_2(^1\Delta_g)$ is, however, possible for Fe. Reaction with O_3 to form MO + O_2 is exothermic for all the metals.

Table VIII lists several reactions which are of interest as possible models for analogous reactions involving metal atoms.

V. Experimental Measurements of Metallic Element Distributions

A. Methods

The metallic elements may be expected to occur in the upper atmosphere in the form of free atoms, as ions (usually of +1 charge) or in the form of low molecular weight molecules or molecular ions (section VIII). Because the concentration of even the most abundant species is very low, detection and estimations of number

(69) L. G. Meira, Jr., *J. Geophys. Res.*, **76**, 202 (1971).

(70) C. R. Philbrick, R. S. Narcisi, R. E. Good, H. S. Hoffman, T. J. Keneshea, M. A. MacLeod, S. P. Zimmerman, and B. W. Reinisch, unpublished observations.

(71) H. C. Wood, Ph.D. Thesis, University of Saskatchewan, Saskatoon, Canada, 1972; see also H. C. Wood, W. F. J. Evans, E. J. Llewellyn, and A. V. Jones, *Can. J. Phys.*, **48**, 862 (1970).

(72) P. J. Crutzen, in "Mesospheric Models and Related Experiments," G. Fiocco, Ed., D. Reidel Publishing Co., Dordrecht, Holland, 1971, pp 78–88.

(73) P. J. Crutzen, private communication. The model reported upon in ref 72 has been modified in several minor respects to take into account newer rate data.

(74) B. G. Hunt, *J. Atmos. Terr. Phys.*, **33**, 1869 (1971).

densities pose very difficult experimental challenges. The experimental results available at present are very scanty. Only the alkali metals, and of these only sodium with any quantitative reliability, have been observed in the free atom form. Several metals have been identified as positive ions (Na^+, Ca^+, Al^+, Mg^+, Cr^+, Fe^+, Ni^+, Si^+). In addition, the molecular ions FeO^+, SiO^+, and—more tentatively—MgO^+ have been reported.

Metallic species in the upper atmosphere have been detected by the following techniques.[75-78]

1. Twilight Airglow

When the sun is below the horizon, the atmosphere directly overhead is illuminated by solar radiation only above a certain altitude, determined by the angle the sun's rays make with the zenith direction. Under these conditions, the background from scattering of solar radiation in the lower atmosphere is absent, and it is possible to observe weak fluorescent scattering from species present in the upper atmosphere. Observations of fluorescent emission in the twilight airglow have provided data on the distributions of sodium, potassium, and lithium atoms,[79,80] and of Ca^+.[81]

2. Dayglow Observations[75]

Resonant scattering of solar radiation in the dayglow can be observed for trace constituents, but the measurements are difficult to make because of the intense scattered sky light from the lower atmosphere. Ground-based observations can be made, however, with instruments of high resolving power. In the case of sodium observations, this high resolving power is attained by using a Zeeman-modulated sodium vapor cell in conjunction with an interference filter.[82,83]

Extensive measurements of sodium distribution have been made for the purpose of determining the details of the diurnal variation. There is some question, however, regarding the magnitude of a correction which must be applied to the data so obtained.[84,85] The correction results from partial filling in of the Fraunhofer lines in scattered sunlight, thus generating a false signal. The magnitude of the false signal may exhibit a diurnal variation,[86,87] which complicates application of a correction to the observed data.

Measurement of the dayglow in a balloon or rocket-borne experiment eliminates much of the contribution from Rayleigh scattered sky light. The rocket experiments furthermore provide more direct data regarding the vertical distribution of the species of interest, since the rocket penetrates the region where the metallic species are most abundant. Rocket-borne measurements have been made of the sodium dayglow[88,89] and of Mg^+.[90]

3. Absorption[75]

It is possible in principle that metallic species might be detected directly by observing their absorption of solar radiation. In practice the absorptions are extremely small and quite undetectable in the presence of the intense background radiation. Atomic sodium is thus far the only metallic species to be seen in absorption.

4. Resonant Scattering of Laser Light

In all of the photometric techniques mentioned thus far, the light source is solar radiation. In recent years it has become possible to excite observable resonant scattering from certain atmospheric species using a tuned laser beam.[91] The technique has been particularly successful in the study of sodium in the night sky. The observations are ground-based; the vertical distribution of the sodium is obtained from time resolution of the signal returned from the laser pulse.[92,93]

5. Nightglow, Auroral, and Meteor Trail Emissions

Sodium emission is observed as an important feature of the nightglow;[75] the source of excitation is not clear, and the measurements do not provide much indication of abundance. Sodium lines have also been observed in emissions from certain types of aurora.[94] In this instance also the source of excitation is not clear; a suggestion of Hunten's,[95] that the excitation may arise from transfer of N_2 vibrational excitation to sodium, does not seem viable in light of recent laboratory experiments,[96] and the matter remains for the time an open question.

Lines characteristic of both neutral and ionized metal atoms have been seen in the emissions from meteor trails.[97] The short-lived emissions are due to species produced during meteoroid ablation.

6. Mass Spectrometry

Rocket-borne mass spectrometers provide information regarding the local concentrations of the species they are designed to measure. Positive ions may be detected directly by a Bennett rf mass spectrometer or a quadrupole instrument.[98,99] The altitude range in which the instrument may effectively operate is determined by the pressure in the sampling chamber. The more recent experiments have employed cryogenic[99,100] or getter system[101-103] pumping to permit measurements as low as 65 km on both upleg and downleg segments of the flight.

Several problems arise in relating the observed ion

(75) A. Vallance Jones, *Ann. Geophys.*, **22**, 189 (1966).
(76) D. M. Hunten, *Space Sci. Rev.*, **6**, 493 (1967).
(77) Reference 15, pp 101–104.
(78) M. Gadsden, *Ann. Geophys.*, **25**, 667 (1969).
(79) D. M. Hunten in ref 11, p 12.
(80) W. A. Gault and H. N. Rundle, *Can. J. Phys.*, **47**, 85 (1969).
(81) A. L. Broadfoot, *Planet. Space Sci.*, **15**, 502 (1967).
(82) J. E. Blamont and T. M. Donahue, *J. Geophys. Res.*, **66**, 1407 (1961).
(83) M. Gadsden and C. M. Purdy, *Ann. Geophys.*, **26**, 43 (1970).
(84) J. Albano, J. E. Blamont, H. L. Chanin, and M. Petitdidier, *Ann. Geophys.*, **26**, 151 (1970).
(85) E. J. Llewellyn and W. F. J. Evans in ref 11, pp 24 and 25.
(86) D. M. Hunten, *Astrophys. J.*, **159**, 1107 (1970).
(87) J. F. Noxon, *Space Sci. Rev.*, **8**, 92 (1968).
(88) D. M. Hunten and T. Wallace, *J. Geophys. Res.*, **72**, 69 (1967).
(89) T. M. Donahue and R. R. Meier, *J. Geophys. Res.*, **72**, 2803 (1967).
(90) J. G. Anderson and C. A. Barth, *J. Geophys. Res.*, **76**, 3723 (1971).
(91) M. R. Bowman, A. J. Gibson, and M. C. W. Sanford, *Nature (London)*, **221**, 456 (1969).
(92) A. J. Gibson and M. C. W. Sandford, *J. Atmos. Terr. Phys.*, **33**, 1675 (1971).
(93) R. D. Hake, Jr., D. E. Arnold, D. W. Jackson, W. E. Evans, B. P. Ficklin, and R. A. Long, *J. Geophys. Res.*, 77, 6839 (1972).
(94) H. Derbloom, *J. Atmos. Terr. Phys.*, **26**, 791 (1964).
(95) D. M. Hunten, *J. Atmos. Terr. Phys.*, **27**, 583 (1965).
(96) H. F. Krause, J. Fricke, and W. L. Fite, *J. Chem. Phys.*, **56**, 4593 (1972).
(97) P. M. Millman and D. W. R. McKinley in "The Solar System," Vol. IV, B. M. Middlehurst and G. P. Kuiper, Ed., University of Chicago Press, Chicago, Ill., 1963, Chapter 21.
(98) F. A. White, "Mass Spectrometry in Science and Technology," Wiley, New York, N. Y., 1968, pp 39–45.
(99) Reference 15, pp 96–98.
(100) A. Johannessen and D. Krankowsky, *J. Geophys. Res.*, 77, 2888 (1972).
(101) R. A. Goldberg and L. J. Blumle, *J. Geophys. Res.*, 75, 133 (1970).
(102) R. A. Goldberg and A. C. Aikin, *J. Geophys. Res.*, **76**, 8352 (1971).
(103) A. C. Aikin and R. A. Goldberg, *J. Geophys. Res.*, **78**, 734 (1973).

currents to the abundances of the ions. Some of the species observed may be contaminants arising in the equipment. In the case of cluster ions, shock-wave effects about the inlet produce heating which may change the composition of the sample before it enters the mass resolution region. Energetic collisions with neutrals resulting from the draw-in potential may also cause disruption of cluster ions. (While these two effects are important in measurements of the hydrated hydronium ion and other clusters below 90 km, they are not of importance for the metal ion measurements above this altitude.) The relative abundances of ions differing greatly in mass may be incorrectly represented because of differing ion speeds in relation to the rocket motion, and because of discriminatory characteristics of the mass spectrometer. Finally, calibration of the measured ion currents in terms of an absolute number density is difficult. Conversion of in-flight data to number densities is normally possible only by equating the total measured positive ion concentration at each altitude above about 90 km to the more accurately measurable electron number density.

The effective mass range for a quadrupole mass spectrometer is limited by various experimental considerations. The height resolution in the measurement of any particular ion is determined by the rocket speed and the recycling time for the mass sweep. The sweep rate must not be made too high since the sensitivity is inversely related to sweep rate. Because much of the interest in the ion composition of the ionosphere has centered on NO^+ and the hydronium ion hydrates, $H_3O(H_2O)_m^+$, many of the instruments flown have not been tailored to detect most effectively heavier metal-containing ions which might be expected to occur.

Assignment of an ion of given mass as a particular chemical entity is not always unambiguous. For example, a mass 28 ion might be either Si^+ or N_2^+; mass 40 might be either Ca^+ or MgO^+. Observations of ions due to isotopically related species in the correct ratio (*e.g.*, $^{24}Mg^+$, $^{25}Mg^+$, $^{26}Mg^+$) can be a helpful indicator. It is especially difficult to distinguish relatively heavy mass peaks which differ by only one or two mass units, *e.g.*, FeO^+ (mass 72) *vs.* $H_3O(H_3O)_3^+$ (mass 73).[100]

Mass spectral observations of neutral species involve the added complication that a source of ionization must be included. The one such study reported to date[70] does not contain results bearing on the abundances of metallic atoms or other metal-containing species.

B. Sodium

The distribution of neutral, atomic sodium has been extensively studied using several of the photometric techniques described above. One must be cautious about placing too fine an interpretation on apparent differences in results obtained by different techniques, at different places and times. Nevertheless, certain features are evident from examination of all the results.

The sodium distribution is rather sharply peaked, with a maximum at about 92 km. The height of the nighttime maximum in mid-latitudes varies seasonally; it is lowest in winter.[92] Measurements at the South Pole indicate a distribution similar to that observed at mid-latitudes.[104] The scale height of the upper part of the layer is invariably found to be 3–4 km or less, considerably smaller than that of the atmosphere in this region.

The total sodium column abundance (*i.e.*, the number of Na atoms in a 1-cm^2 column reaching to the top of the atmosphere) is found in all the various measurements to occur in the range 2×10^9–2×10^{10} atoms cm^{-2}. The distribution shows a winter enhancement at mid-latitudes.[76,80,92] Figure 6 shows data for the nighttime distribution over the period of a year, based on laser light-scattering measurements.[92] These results exhibit the characteristic sharp peaking in the distribution, a seasonal variation in the height of the maximum, and the winter enhancement. Gadsden reports, by way of contrast, that the seasonal variation in abundance is not so marked at the South Pole,[104] on the basis of twilight airglow results.

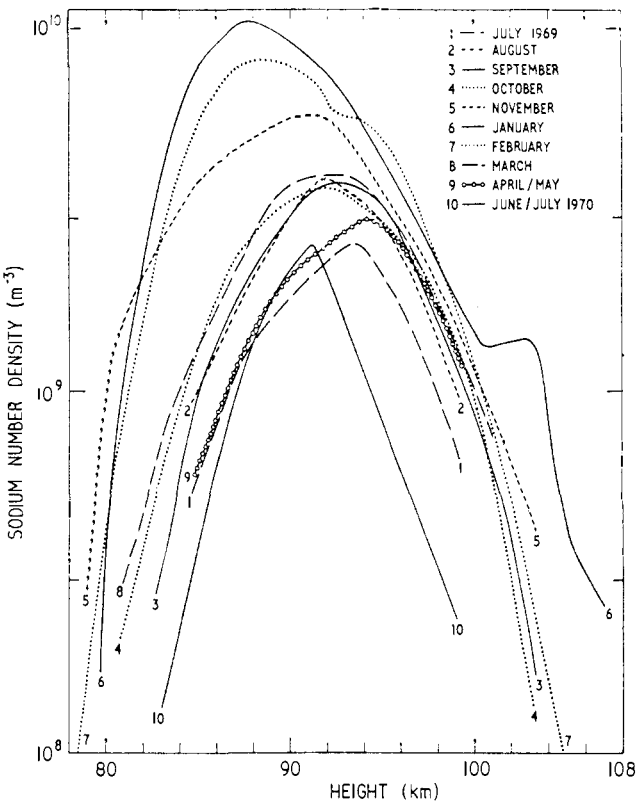

Figure 6. Distribution of Na during a 1-year period, based on pulsed laser echo experiments.[92]

The dayglow measurements, both ground-based[83,84] and rocket-borne,[89] indicate a marked diurnal variation. The abundance increases rather markedly during the first few hours after sunrise, to a maximum at some time after noon, then declines to an evening twilight value about the same as the original morning twilight value. The daytime enhancement may be related to an observation based on satellite results,[105] of large enhancement in the dayglow over each pole in the period around local midsummer. It is rather disturbing, on the other hand, that an extensive series of daytime absorption measurements[106] indicates much smaller diurnal variations than observed in the dayglow studies. Furthermore, recently completed daytime measurements using resonance scattering of a tuned laser pulse[107] show no evidence of a daytime enhancement. The discrepancy remains unresolved at present, although the newer and perhaps more reliable laser measurements strongly indicate lack of a daytime variation. The variation in sodium abundance during nighttime is quite small, if indeed there is any,[92] during normal conditions. Recent laser pulse experiments[93] have shown a

(104) M. Gadsden, *Ann. Geophys.*, **25**, 721 (1969).

(105) T. M. Donahue, B. Guenther, and J. E. Blamont, *EOS, Trans. Amer. Geophys. Union*, 51, 587 (1970).

(106) C. R. Burnett, W. E. Lammer, W. T. Novak, and V. L. Sides, *J. Geophys. Res.*, 77, 2934 (1972).

(107) A. J. Gibson and M. C. W. Sandford, *Nature (London)*, **239**, 509 (1972).

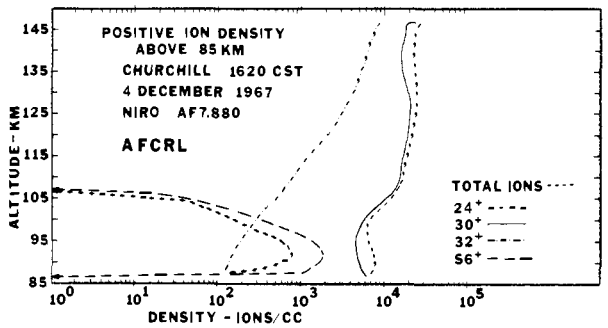

Figure 7. Positive ion densities of the major ions in the E region (R. S. Narcisi, by permission).

very interesting increase in the Na level during the early night, during a period of Geminid meteor shower activity.

Sodium ion has been detected in positive ion mass spectrometer experiments.[108-110] The ion distribution peaks at around 93 km; it is a relatively small component of the total observed metal ion concentration in this region. The altitude density distribution is found to be similar to that for neutral sodium, insofar as the rather rough mass spectral data permit comparison. The Na^+ concentration at maximum is on the order of 10^2–10^3 cm^{-3}.

C. Other Alkali Metals

Both K and Li emissions have been observed in the twilight airglow.[80,111] The most recent work[80] suggests that the vertical distributions are similar to the Na distribution. There does not appear to be much seasonal variation in the K distribution. The abundances of K and Li are much lower than for Na. The ratio of densities Na:K:Li is estimated[112] to be about 1000:5:1. Attempts to detect K in the dayglow have been unsuccessful.[84] The Li abundance appears to vary sporadically,[80,113] which suggests that contamination from artificial sources is a significant component.[75]

D. Magnesium

Neutral Mg atoms have been clearly identified in the spectra of meteors.[97] On the other hand, emission from Mg was not detected in an experiment involving a rocket-borne ultraviolet spectrometer flown into a sporadic E layer.[90] In that experiment, emission from Mg^+ was observed; the column density was estimated at 4×10^9 cm^{-2} with a peak ionization at 108 km, based on ground-based ionosonde data. Gadsden[114] has suggested, however, that the column abundance of Mg calculated by Anderson and Barth could be too low, by a factor of perhaps 20. The first observation of Mg^+ using a rocket-borne positive ion mass spectrometer was made by Istomin in 1963.[115] He estimated that the Mg^+ maximum occurred at 105 km and that the column abundance was 7×10^9 cm^{-2}. The Mg^+ abundance and distribution have been observed in considerably more detail and under various conditions in several subsequent rocket studies, most notably those by Narcisi and coworkers.[15,70,108,110,116] The identification of mass 24 as due to Mg^+ is made more certain by the observation of the mass 25 and 26 isotopes, present in terrestrial material to the extent of 10.1 and 11.3%, respectively.

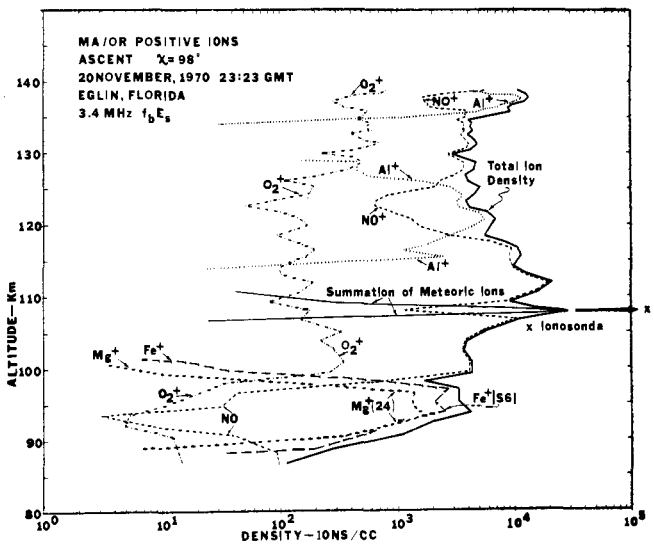

Figure 8. Positive ion composition during a sporadic E layer occurrence.[70] The Al^+ layers are due to release of $Al(CH_3)_3$ from another rocket launched 4 min before the mass spectrometer payload. The depletion of NO^+ (and to a lesser extent of O_2^+) at the altitudes of the Al^+ layers is presumably due to charge-transfer reaction with neutral Al species.

In general, Mg^+ occurs in comparable abundance with Fe^+ and exhibits a closely similar altitude profile. Even in the absence of strongly disturbing conditions (such as a meteor shower), the Mg^+ profile exhibits a strong maximum at about 90–95 km with a width at half-density on the order of 5–10 km (Figures 7 and 8). When a sporadic E layer condition exists, the estimated metal ion density in the region of the Mg^+ and Fe^+ maximum constitutes a large fraction (on the order of 60%) of the total positive ion density.[70,109,110,116,117] The Mg^+ concentrations in the region of the maximum are on the order of 10^3–10^4 cm^{-3}.

A second, narrower and denser layer of meteoric ions is frequently found near 108 km altitude. This layer, which is the one most closely identified with the sporadic E phenomenon (see section VI), is invariably found to contain Mg^+, although its abundance relative to the other metallic ions is different from that in the layer at 90–95 km. The Si^+ ion is usually the predominant ion in the higher layer, whereas it is normally not seen at all in the lower layer (*vide infra*).

In an experiment launched at noon into the 1965 Leonid meteor shower, Narcisi[116] observed Mg^+ in somewhat higher concentration than Fe^+ in a maximum at 97 km and estimated the total metal ion concentration at the maximum to be on the order of 10^4 cm^{-3}. A second layer was observed at 111 km, in which the relative concentrations were in the order $Si^+ > Fe^+ > Mg^+$. A positive ion composition measurement at evening twilight from the same location, at the same time of year,[70] through a sporadic E layer at 108 km showed a substantial peak with Mg^+ and Fe^+ in comparable concentrations, $>10^3$ cm^{-3} at 95 km, and a much more intense meteoric ion layer consisting primarily of Si^+, with a total metal ion concentration of about 10^5 cm^{-3} at 108 km (Figure 8). Although it is not possible to make detailed

(108) R. S. Narcisi, *Ann. Geophys.*, **22**, 224 (1966).
(109) R. S. Narcisi, A. D. Bailey, and L. Della Lucca, *Space Res.*, 7, 446 (1967).
(110) R. S. Narcisi, A. D. Bailey, and L. Della Lucca, *Space Res.*, 7, 123 (1967).
(111) H. M. Sullivan and D. M. Hunten, *Can. J. Phys.*, **42**, 937 (1964).
(112) H. N. Rundle in "The Radiating Atmosphere," B. M. McCarmac, Ed., D. Reidel Publishing Co., Dordrecht, Holland, 1972, pp 100, 101.
(113) H. M. Sullivan, *Ann. Geophys.*, **26**, 161 (1970).
(114) M. Gadsden, *J. Geophys. Res.*, **77**, 1330 (1972).
(115) V. G. Istomin, *Space Res.*, **3**, 209 (1963).
(116) R. S. Narcisi, *Space Res.*, **8**, 360 (1968).
(117) J. M. Young, C. Y. Johnson, and J. C. Holmes, *J. Geophys. Res.*, **72**, 1473 (1967).

comparisons, these particular results, which are not atypical, suggest that the metal ions, particularly Mg^+ and Fe^+, occur in a fairly regular distribution. The experiments reported by Narcisi and coworkers were carried out for the most part at a mid-latitude location (Elgin, Florida), but the available data suggest that a similar distribution prevails at other latitudes. An experiment from Fort Churchill, Canada, fired into an active aurora,[108] showed a Mg^+ maximum at about 100 km. More recently[100] an experiment launched from Andoya, Norway, in August 1971, and which reached a peak altitude of only 99 km, showed a maximum in Fe^+ and Mg^+ (10^3–10^4 cm^{-3}) at about 90 km.

Aside from Mg^+, no other magnesium-containing ions have been unambiguously identified in the positive ion composition measurements. An ion of mass 40 often seen in the vicinity of the metal ion maxima at 90–95 and 110 km has been attributed[100,108] to Ca^+. It is possible *a priori* that this species is in fact MgO^+, but chemical considerations suggest that MgO^+ should have low abundance relative to Mg^+ (*vide infra*). Because the ion occurs in concentrations on the order of only 10^2 cm^{-3}, at the threshold of observability, it has not been possible to test the presence of Mg by determining the presence or absence of the isotopically related ions. The identity of the mass 40 ion therefore remains uncertain for the moment.

E. Calcium

Emission from neutral calcium atoms has been clearly identified in the spectra of meteors;[97] Ca^+ is also seen, but less strongly. Resonance scattering of sunlight from Ca^+ has been observed as a weak, sporadic feature of the twilight airglow.[75,81,118] The most recent and extensive measurements due to Broadfoot[81] suggest that the observed Ca^+ is distributed throughout the altitude range 100–180 km rather than strongly layered. The observations correlate reasonably well with increased meteor activity during the spring and summer months. Twilight-glow measurements of such a weak feature do not permit measurements below about 100 km, so the presence of Ca^+ layer in the region of 95 km cannot be determined by this technique. There is, however, no evidence in the measurements for a layer at 110 km, where mass spectral measurements reveal an ion of mass 40, assigned to Ca^+.[100,108,115] The number density at maximum estimated from the mass spectral data for the mass 40 ion at 94 km is on the order of 10^2 ions/cm^3, with an indication of considerably higher number densities above 110 km. But it has been estimated that a Ca^+ number density of about 2.5×10^2 cm^{-3} over a 10-km interval in the vicinity of 110 km should provide an easily detectable scattering layer, whereas none was observed in the course of the measurement program.[81] The mass 40 ion observed in the mass spectral experiments may therefore not be due to Ca^+. Resonant scattering from neutral Ca, which has a strong resonance line at 422.7 nm, has not been observed in the twilightglow.[75,78] It is noteworthy that Gadsden reports failure to observe resonant scattering from either Ca or Ca^+ in twilight airglow experiments conducted at the South Pole.[78] He places an upper limit on the Ca^+ column abundance of about 0.3×10^8 cm^{-2}, which is smaller than the column abundances implied in Broadfoot's observations. Although Broadfoot's observations were made in the mid-latitude (Kitt Peak Observatory, Tucson, Arizona, 40°N), the influx of meteoroids which is presumed to give rise to the Ca^+ is not expected to change markedly with latitude. Gadsden estimates[38] that the deposition rate averaged over a day is only about 17% less at 90° as compared with 0° latitude. The discrepancy probably arises in experimental considerations. Broadfoot obtained his best signal/noise ratios for the Ca^+ emission for solar depression angles of 10–20°, much larger than Gadsden was able to manage in the course of his observational program. The competition from atmospheric background when working at solar depression angles of 7–4° could effectively preclude observation of Ca^+, even though the observation times are longer.

F. Iron

Emissions from neutral iron atoms are seen very clearly in meteor spectra.[97] On the other hand, emissions from Fe^+ are so faint as to be of questionable origin. Aside from meteor spectra, no iron in any chemical form has been observed in the ionosphere by spectroscopic means. The only reported attempt is due to Gadsden,[78] who searched unsuccessfully for the Fe resonance line at 385.9 nm in the twilightglow at the South Pole. He estimates upper limits for the Fe column abundance of about 8×10^8 cm^{-2} in autumn and about twice this in the spring.

Positive ion mass spectral studies reveal the ion of mass 56 assigned to Fe^+, as a major component of the "metallic layers"[15,70,100,108,110,116,119] (Figure 7). Although this mass might conceivably be due to another species, there are strong arguments for assigning it as Fe^+. (a) It is closely related, in terms of relative intensity and vertical distribution in the 90–95-km range, to the +24 ion which can be assigned to Mg^+ on the basis of isotopic distribution. (b) The prevalence of an unusually high abundance of ions assigned as metallic is relatable to the occurrence of unusually heavy meteor showers,[15,103,116] and the relative abundances are in rough general agreement with the compositions of chondritic meteorites which strike the earth. (c) On some of the telemetry records a peak assignable to the mass 54 nuclide of Fe (5.8% abundance) is visible.[103,120]

The mass 56 ion assigned to Fe^+ frequently exhibits two abundance maxima, at 90–95 and 105–115 km. As shown in ref 116, Figure 1, the metal ion maximum at 98 km, which is about 40% Fe^+, is essentially the same on both ascent and descent. The measurements in this instance were separated horizontally by 21 km and by about 2 min in time. Narcisi reports[116] that the ratio Mg^+/Fe^+ is about 0.5 both above and below the maximum, and about 1.3 within the layer.

The results exhibited in Figure 8 were taken shortly after sunset. Again, the agreement between ascent and descent data is excellent. It is noteworthy that in the 90–95-km region the metallic ions dominate the positive ion distribution, a relatively common occurrence at night, when NO^+ and O_2^+ levels are lower. In general, the appearance of strongly layered metallic ion maxima at 90–95 km and at 105–115 km is associated in mid-latitudes with sporadic E layer formation.[121-122] (The relationship of the metallic ions to sporadic E layer formation is discussed in section VI.) Under these conditions the metallic ions dominate the positive ion distribution in the vicinity of the layer or layers. The Fe^+ concentration at

(118) N. Hun-Doan, *Ann. Geophys.*, **22**, 599 (1966).

(119) D. M. Thomas, R. S. Narcisi, A. D. Bailey, and L. E. Wlodyka, *EOS, Trans. Amer. Geophys. Union*, **53**, 456 (1972).

(120) R. S. Narcisi, C. R. Philbrick, A. D. Bailey, and L. Della Lucca, ref 46, p 355.

(121) W. I. Axford and D. M. Cunnold, *Radio Sci.*, 1, 191 (1966).

(122) Reference 1, p 365.

maximum is then usually in the range 10^3–10^4 ions/cm^3. Even when strong layering is not observed, however,[100,103] and when NO^+ and O_2^+ levels exceed those of the metals, the metal ions are observed to occur in a broad maximum in the range 90–95 km, and with Mg^+ and Fe^+ concentrations on the order of 10^3 ions/cm^3.

The opportunities for detailed comparisons of the metal ion concentrations in the vicinity of 110 km with those in the 90–95-km range have been rare because several of the rockets flown have reached peak altitudes below 110 km. The magnitudes and altitudes of the higher layer do appear, however, to be more variable than for the more stable lower layer.

The presence of Fe^+ at much higher altitudes has recently been claimed on the basis of measurements made from the Ogo 6 satellite.[123-125] An ion trap in the satellite is sensitive to the mass of an ion which strikes it because of the supersonic motion of the satellite through the atmosphere. Hanson and Sanatini were able to obtain significantly better fits to the curve of ion trap current *vs.* retarding potential by assuming the presence of an ion with a mass of 56, with good sensitivity of the fit to assumed mass number as well as number density. The detectability threshold is estimated to be 4 ions/cm^3. They assign the mass 56 ion as Fe^+. The ion is observed over an altitude range from 1000 km to as low as about 400 km with variable abundance. Most of the reported data refer to altitudes between 600 and 450 km. Although Fe^+ concentrations as high as 2000 cm^{-3} are claimed, the more usual levels are on the order of 10^2 cm^{-3} or less.

It is hypothesized that Fe^+ ions formed in the range 100–120 km are relatively long-lived ($\gg$1 day) and that they are borne upward in current drifts with velocities on the order of 60 km/hr. The authors found evidence for a lighter mass ion in concentrations comparable to the +56 ion. Although this might logically be expected to arise from Mg^+, an assumed mass of 30 gave the best fit with the observations.

These results raise several interesting questions. If the +56 species is due to Fe^+, as assumed, is the total influx of metal ion *via* meteor ablation in the 100–120-km range sufficient to provide the required Fe levels? What is the eventual fate of the Fe^+? How can the assumption that the heavy ion is Fe^+ be reconciled with the difficulty in fitting the lower mass ion to Mg^+ or Si^+, which are of comparable abundance in the 120–90-km range?

G. Other Elements

Several metallic elements are observed in the spectra of fast meteors.[97] Aside from these observations there is no evidence from optical experiments for metallic elements in the ionosphere other than those discussed in the preceding sections.

It is especially significant that neither Si^+ nor SiO^+ is very abundant in the 90–95-km range in which Mg^+ and Fe^+ show a maximum. On the other hand, Si^+ is the most abundant component of the layer at 110 km;[70,116] SiO^+ is also seen in this layer in lower abundance. Narcisi has suggested[108] that a mass 28 ion seen in the altitude range 64–82 km may be Si^+, since it is extremely unlikely that N_2^+ could exist at measurable levels in this altitude range. The observation, made in one of the earlier experiments, may have been spurious, since it has not been repeated in any of the several subsequent rocket experiments.

Al^+, Ni^+, and Cr^+ have been reported as minor components of the positive ion mass spectrum in the 90–95-km range.[116]

VI. Mid-Latitude Sporadic E Layers

Transient thin spikes in the normal E region electron profiles, referred to as sporadic E layers, are found at all latitudes. Those occurring in the mid-latitude range are related to the behavior of the metallic ions which, as we have seen, are found to occur in narrow layers in the range from about 90 to 120 km.

Layering of the metallic ions has been related theoretically to the existence of wind shears in the ionospheric region.[121,126,127] The origin of these wind shears need not concern us here; it is sufficient to note that there is extensive experimental evidence for horizontal east–west winds which alternate in direction over a relatively narrow altitude range.[128,129] Thus, for example, at any given time one might have a strong west wind at say 80 km, gradually decreasing in magnitude with increasing altitude, a null in the wind at say 95 km, then an increasingly strong east wind at altitudes above the null. The alternation in wind direction occurs with a periodicity in the vertical direction of perhaps 20–30 km. These horizontal east–west winds move the neutral atmosphere, and the ions along with it, across the lines of the earth's geomagnetic field.

Charged particles moving with velocity **v** normal to the lines of the earth's magnetic field, **B**, are subject to a Lorentz force $e(\mathbf{v} \times \mathbf{B})$. In the absence of collisions with other particles, a charged particle moving with a constant velocity component normal to the earth's magnetic field lines would describe a circular motion of radial frequency $\omega = eB/m$. Clearly, this gyro frequency, as it is called, is much greater for the electron than for a heavy positive ion such as Fe^+, for example. In the absence of frequent collisions, therefore, the charged particle would simply revolve around a magnetic field line. Positive ions and electrons in the atmosphere at high altitudes, above about 140 km, undergo sufficiently infrequent collisions with neutral atmosphere particles so that this state of affairs applies to them. They are essentially trapped on a magnetic field line, and a horizontal wind does not effectively move them in the east–west directions. At much lower altitudes, where the collision frequency Z of the positive ions with particles of the neutral atmosphere is very much greater than the gyro frequency ($Z/\omega > 10$), the neutral atmosphere exerts a drag on the vertical motion of the positive ion; it simply follows the neutral wind. The interesting region lies between these two extremes, where $0.1 < Z/\omega < 10$. In this region, the positive ions are able to follow the neutral wind in horizontal displacement at perhaps half the velocity, but, in addition, a persistent, unidirectional vertical component of motion is acquired. Thus, a wind blowing toward the east across the geomagnetic field lines produces an upward movement of the positive ions, whereas a wind blowing toward the west produces a downward motion (see Figure 9). Because of the electric fields established by the motions of the positive ions, the electrons are constrained to follow the movement of the positive ions to maintain electrical neutrality within any given volume of atmosphere.

(123) W. B. Hanson and S. Sanatani, *J. Geophys. Res.*, **75**, 5503 (1970).
(124) W. B. Hanson and S. Sanatani, *J. Geophys. Res.*, **76**, 7761 (1971).
(125) W. B. Hanson, D. L. Sterling, and R. F. Woodman, *J. Geophys. Res.*, 77, 5530 (1972).
(126) J. D. Whitehead, *J. Atmos. Terr. Phys.*, **20**, 49 (1961).
(127) T. J. Keneshea and M. A. MacLeod, *J. Atmos. Sci.*, **27**, 981 (1970).
(128) N. W. Rosenberg and C. G. Justus, *Radio Sci.*, 1, 149 (1966).
(129) N. W. Rosenberg, *Radio Sci.*, 1, 246 (1966).

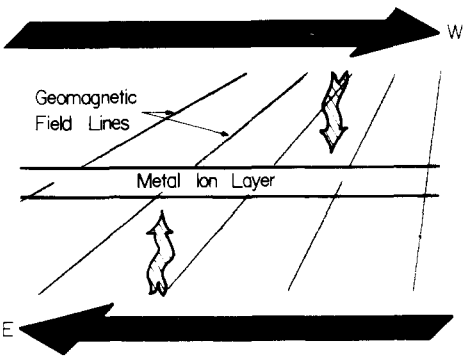

Figure 9. Schematic illustration of sporadic E layer formation via a wind shear.

If the vertical profile of the east-west wind structure has periodic character, as shown in Figure 10,[128,129] then more than one metal ion layer may be seen within the region of atmosphere where layering is permitted by the considerations mentioned above. Furthermore, there is evidence that the periodic wind structure has a downward phase velocity,[128] so that the nulls at which the metal ions collect may move downward. The metal ion layers will thus follow the nulls,[130] until an elevation is reached where the collision frequencies become too high, and the ions are no longer able to keep up. The metal ion layer is then left behind, as it were, by the wind structure, to dissipate by diffusion. This may be expected to occur in the vicinity of 80–90 km altitude.

Why does the layering induced by the wind shears involve principally the metallic ions? Why do NO^+ and O_2^+, which are important ions in this region, not also collect in layers to a similar extent? The answer is that the time scale for formation of a layer is on the order of several minutes to a few hours. Since only a small fraction of the O_2 and NO is ionized, once the ion is neutralized, even assuming that it retains its molecular identity, it would remain neutral for a long time before returning to the ionized state. It follows that a given O_2^+ or NO^+ ion, once ionized, must remain ionized for a long time if it is to experience layering. But the average lifetime of NO^+ and O_2^+ is quite short in the D and lower E regions because of rapid dissociative recombination. These species therefore do not experience significant layering. The metal ions, on the other hand, are assumed to possess long average lifetimes and are thus susceptible to layering as described above. While the wind shear theory plausibly accounts in a general way for the observed phenomena, it relies upon several unproven assumptions. A clear experimental verification of the relationship between ionospheric winds and sporadic E layer formation has been lacking. Indeed, there is some evidence that layering occurs precisely where the wind shear theory predicts it should not.[131-133] The interested reader is referred for further insights to a series of recent papers dealing with mid-latitude Sporadic E.[134]

VII. Origin of Ionospheric Metals

The origin of the metallic elements observed in the ionosphere has been the subject of much speculation.

(130) G. Chimonas and W. I. Axford, *J. Geophys. Res.*, **73**, 111 (1968).

(131) N. W. Rosenberg, H. D. Edwards, and J. W. Wright, *Space Res.*, **4**, 171 (1963).

(132) N. W. Rosenberg and H. D. Edwards, *J. Geophys. Res.*, **69**, 2819 (1964).

(133) E. B. Dorling, K. Norman, and A. P. Wilmore, *Planet. Space Sci.*, 17, 1207 (1969).

(134) See *Radio Sci.*, 7, 345–432 (1972).

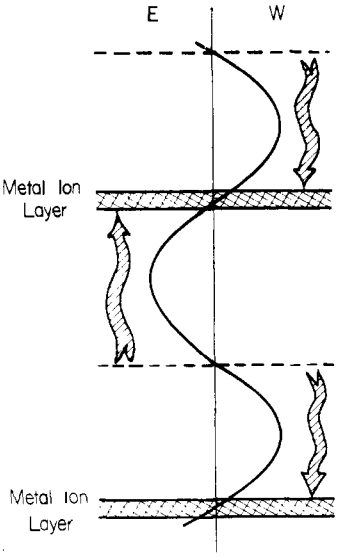

Figure 10. Periodicity of ionospheric winds. The solid sinusoidal curve represents the varying magnitude and direction of the wind with altitude. Metallic ion layers collect at the alternate nodes. The geomagnetic field lines are directed out of the plane of the figure, with North in the direction of the reader. The periodic wave propagates downward, carrying the metal ion layers to lower altitudes. It should be noted that a constant east-west component of wind extending over the entire altitude range might be superimposed on the periodic feature without essentially changing the picture.

Hypotheses regarding source may be broadly divided into those which involve an extraterrestrial origin and those which suppose that the metals originate from the earth's surface. Because the data are fragmentary, it is difficult to present a strong argument against one or the other model on the basis of relative abundances, or temporal variations in abundance and distribution.

Hypotheses of a terrestrial origin generally assume that the major source of the metals is particulate matter from evaporated sea spray, carried to high altitudes by intense stratospheric warming during the polar night.[135] The seasonal variation in the sodium layer, which shows a maximum column abundance during winter, is consistent with such a mechanism. On the other hand, it is not clear that salt particles can yield atomic sodium or magnesium, in either the form of neutral atoms or singly charged ions.[135,136] Furthermore, although conclusive arguments regarding origin cannot be made with respect to the alkali and alkaline earth elements, the presence of iron is not accountable in terms of a marine origin.

The most generally plausible hypothesis thus seems to be that the bulk of the metallic species seen has its origin in extraterrestrial material. Given this assumption, however, there remains the question of whether the atoms and ions observed arise from evaporation of meteoric material which is in the appropriate range of particle size to heat strongly on entering the earth's atmosphere, ablating to (mainly) atoms. The relative velocities of particles which enter the earth's atmosphere and which are themselves in orbit around the sun must lie between about 11 and 72 km sec^{-1}. The majority of meteoroids are in orbits near the ecliptic (the plane of earth's rotation about the sun), and moving in the same direction as the earth,[137,138] so the velocity distribution is skewed toward the 15–20 km sec^{-1} range. Extensive studies

(135) E. R. Allen, *J. Geophys. Res.*, 75, 2947 (1970).

(136) A. E. Potter, Jr., ref 46, p 240.

(137) M. Gadsden, *J. Atmos. Terr. Phys.*, **30**, 151 (1968).

(138) B. L. Kascheev, V. N. Lebedinets, and M. F. Lagutin, "Meteoric Phenomena in the Earth's Atmosphere," Nauka, Moscow, 1967.

have shown that at these relative velocities the particles ablated from meteoroids should be predominantly atoms rather than ions (section II.B), consistent with meteor observation data.[97] The ablation process is confined to a rather narrow range of altitude, with a maximum rate of ablation per unit height interval in the vicinity of about 90 km for a 15-20 km sec^{-1} particle of approximately 10^{-2} cm radius.[137] For more energetic particles the height of maximum ablation is increased. The model on which these conclusions are based contains many assumptions which may be incorrect in detail, but it is clear that ablation of meteoroids with widely varying radii and relative velocities should occur in the altitude interval around 90-120 km.

The quantity of matter deposited in the ionosphere through ablation of meteoroids has been estimated by Gadsden[137] as 9×10^{10} g $year^{-1}$. On the basis of entirely different considerations from those used by Gadsden, Hughes[139] has recently estimated the annual influx as about 5×10^{8} g $year^{-1}$. The higher figure, which is far from the highest estimates,[89] corresponds roughly to a column influx of about 2×10^{6} metallic atoms cm^{-2} sec^{-1}.

Gadsden[140] has outlined a model for the distribution of metallic elements in the ionosphere, taking account of the deposition of atoms from ablating meteors, and assuming relatively rapid ionization of the atoms *via* charge-transfer processes. The model includes in a simplified way diffusion and the downward sweeping of the metallic ions *via* a neutral wind mechanism as described in section VI. Layering of the ions as a result of a wind shear is, however, neglected. He concludes that the model is capable of reproducing the general form of the sodium atom distribution, by assuming a particular amount and type of meteor influx into the atmosphere. Diffusion processes appear as a dominant factor in determining the distribution.

As an alternative hypothesis, it has been suggested[89,112] that atoms may result from an aerosol of particles with radii $< 10^{-6}$ cm, resident in the ionosphere for a time on the order of several years. The constituents of such an aerosol might originate from any source, terrestrial as well as extraterrestrial. The aerosol is assumed to be in a dynamic equilibrium with the gas-phase species and to maintain a size-weighted distribution as a result of eddy diffusion. Although such a model has many attractive features, it is not at all clear that it can be sustained in terms of chemical considerations. Fiocco and Visconti[141] have recently described an attempt to account for the seasonal variation in the sodium column abundance in terms of an evaporation model. They appear to have chosen the evaporation of sodium from sodium metal in estimating the rate of evaporation and its temperature dependence. It does not seem at all plausible, however, that sodium should exist as the solid metal under the chemical conditions which obtain at 90-95 km.

Much of the discussion regarding various hypotheses of origin has developed in an attempt to account for the extensive observational data on the sodium atom layer. Even if the observational results on which the discussions have been based could be assumed to be correct, there is little basis for preferring one model over another. In any case, the recent laser radar results,[92,107] which seem to indicate the absence of a regular diurnal variation, and the more recent evaluations of the height distributions of the other alkali and alkaline earth metals, have altered the considerations considerably.

(139) D. W. Hughes, *Planet. Space Sci.*, **20**, 1949 (1972).
(140) M. Gadsden, *Ann. Geophys.*, **26**, 141 (1970).
(141) G. Fiocco and G. Visconti, *J. Atmos. Terr. Phys.*, **35**, 165 (1973).

TABLE IX. Relative Abundances of Ionospheric Ions and Neutral Elements in Chondrite Meteorites (Si = 100)

Element	Ion (114 km)[145]	Chondrites[146]
Na	9.1	4.3
Mg	57	96
Si	100	100
K	0.38	0.30
Ca	1.2	5.5
Sc	0.35	0.003
Cr	1.77	1.1
Fe	158	74
Ni	4.7	3.9

It is the opinion of the writer that the most plausible hypothesis of origin at present is that the metallic elements arise *via* ablation of meteorids entering the earth's atmosphere. Despite the rather fragmentary evidence, it does appear that the relative abundances of sodium, magnesium, iron, nickel, calcium, and aluminum are roughly consistent with a meteoric origin.[142-144] A tiny fraction of the solid material which impinges on the earth's atmosphere survives the intense heating which accompanies deceleration. The lumps of extraterrestrial material which land on the earth's surface are termed meteorites. They constitute the only available evidence regarding the composition of material which is in the size range for complete ablation in the upper atmosphere. It is not certain that the meteoritic material is representative of all the material which contributes to the metallic elements in the ionosphere, but it seems reasonable to assume that this is the case.[144a]

About 92% of the known meteorites are classified as stones, and most of these in turn are classified as chondrites. The stones consist largely of silicate minerals containing predominantly Fe^{2+} and Mg^{2+}, and Na^{+}, Ca^{2+}, and other metals in lesser amounts. About 6% are predominantly iron metal, with some nickel. About 2%, termed stony irons, contain a mixture of iron metal and silicate minerals.

Evidence for a meteoric origin comes from correlations of ionospheric metal levels with meteor activity. Positive ion mass spectral observations taken during periods of heavy meteor shower activity clearly indicate exceptionally heavy incidences of the metallic ions.[116] Goldberg and Aikin have recently reported[145] the results of a rocket-borne ion mass spectrometer experiment launched at the time of growth of a sporadic E layer, during a period in 1972 of the β Taurids meteor shower. The β Taurids showers are not especially intense; they result in increases of only a few per cent in the flux of extraterrestrial material. Nevertheless, there was evidence of enhanced metallic ion densities, and a well-defined metallic ion peak was observed at 114 km (Figure 11). Table IX shows the relative abundances of the metallic ions observed in the mass spectrometric experiment, as compared with the elemental composition of chondrites. The relative abundances of the elements compare reasonably well, although the abnormally high abundance of the mass 45 ion, assigned to Sc, is puzzling.

(142) E. Anders, *Space Sci. Rev.*, **3**, 583 (1964).
(143) E. Anders, *Accounts Chem. Res.*, 1, 289 (1968).
(144) B. Mason, Ed., "Handbook of Elemental Abundances in Meteorites," Gordon & Breach, New York, N. Y., 1971.
(144a) B. Baldwin and Y. Sheaffer, *J. Geophys. Res.*, **76**, 4653 (1971).
(145) R. A. Goldberg and A. C. Aikin, *Science*, **180**, 296 (1973).
(146) The elemental abundances listed for chondrites are based on data from ref 144, and are relative number abundances. The values listed by the authors in ref 145 for comparison with their experimental data are on a weight basis.

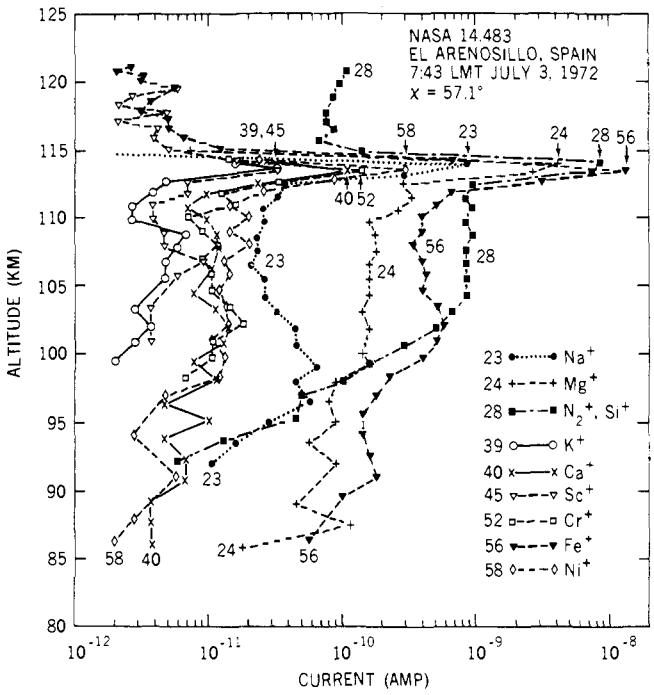

Figure 11. Daytime positive ion profiles during a weak meteor shower and during sporadic E layer growth.[145]

The reported absence of a correlation between the sodium atom column abundance and meteor activity is possibly related to the time scale for development of the neutral atom layer and the nature of factors which dominate in controlling its form. In this connection, however, it should be noted that the most recent pulsed dye laser studies[93] of the Na layer show an apparent increase in the column abundance during the hours after twilight, reaching a maximum in the early morning. These observations were made during a period in which there was unusually heavy (Geminid) meteor activity. This point will be returned to in section IX following presentation of the results of the chemical model.

VIII. A Chemical Model

Aspects of the chemistry of the metallic elements in the ionosphere have been considered previously by several authors (ref 22, 54, 76, 82, 90, 103, 147–152). Figure 12 shows in schematic form a generalized outline of the chemical processes which might *a priori* be of importance for any one of the metallic elements. Not all of these reactions will be operative for a given element. Further, a particular part of the scheme will dominate the chemistry in one altitude region but be of no importance in another.

Eight species which may appear in the distribution of metals among various chemical states are included in the scheme. Aside from the singly charged metal ion, the cluster ions with both oxygen and nitrogen, MO_2^+ and MN_2^+, respectively, can be expected to play an important role. Reaction of M^+ with either O (in a three-body process) or with O_3 leads to MO^+. Reaction of this species with O leads back to M^+. Alternatively, the cluster ions might react with O or O_3 to form MO^+. (In point of fact, the reaction of the cluster ions with O_3 can be neglected because the positively charged species are of importance only above about 90 km, where $O \gg O_3$ at all times.)

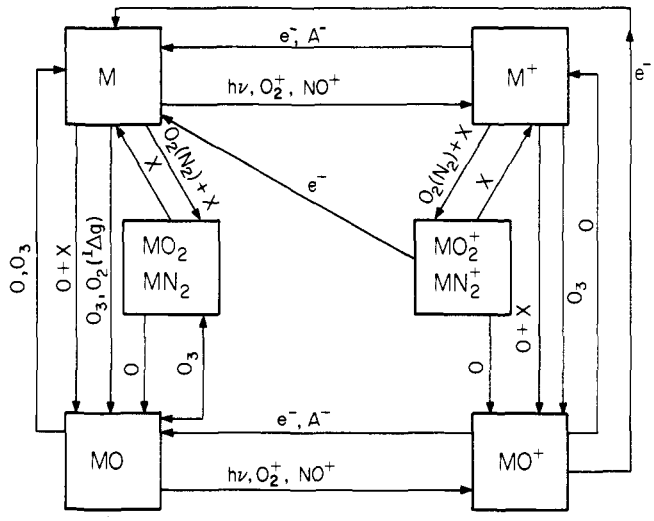

Figure 12. Schematic representation of metallic element chemistry in the mesosphere and ionosphere.

The chemical "map" shown in Figure 12 is essentially symmetrical with respect to the correspondence between charged and neutral species. The neutral metal atom is also capable of reaction with either O (in a three-body process), O_3, or $O_2(^1\Delta_g)$ to form MO, which is recycled back to M *via* reaction with O. The neutral atoms are also capable of forming clusters in a three-body reaction with either N_2 or O_2. Not much attention has been paid to these reactions, which are of potentially great significance.

Andrews has shown that the lithium atoms interact with O_2 to form an MO_2 species which he has characterized *via* matrix isolation studies.[153] The corresponding species with N_2 may be expected to be much less stable.[154] Indeed, it seems unlikely that the free energy of formation of MN_2 would be sufficiently large for these species to be of interest for nontransition metals under the conditions which obtain in the mesosphere. For the transition metals, on the other hand, there is good reason to suppose that the MN_2 species are of sufficient stability to be of importance.

Transition metal complexes of dinitrogen have been known for several years, since the first report by Allen and Senoff[155] of the $Ru(NH_3)_5N_2^{2+}$ ion. A large number of N_2 complexes of transition metals in low and formally zero charge states are now known.[156,157] The N_2 molecule is observed to coordinate in a linear fashion, in the manner of CO. The stability of the N_2–metal interaction is generally accounted for in terms of a bonding model similar to that employed in explaining the bonding of CO; *i.e.*, the N_2 is assumed to act as a σ donor toward the metal and as a π acceptor.

Turner and coworkers[158] and Ozin and coworkers[159] have recently reported the formation of dinitrogen com-

(147) W. Swider, *Ann. Geophys.*, **26**, 595 (1970).
(148) J. E. Blamont and T. M. Donahue, *J. Geophys. Res.*, **69**, 4093 (1964).
(149) H.-R. Lehmann and C. U. Wagner, *J. Atmos. Terr. Phys.*, **28**, 617 (1966).
(150) R. R. Burke, J. Geophys. Res., **75**, 1345 (1970).
(151) R. R. Burke, *J. Geophys. Res.*, 77, 1998 (1972).
(152) E. E. Ferguson, *Radio Sci.*, 7, 397 (1972).
(153) L. Andrews, *J. Chem. Phys.*, **50**, 4288 (1969).
(154) R. C. Spiker, Jr., L. Andrews, and C. Trindle, *J. Amer. Chem. Soc.*, **94**, 2401 (1972).
(155) A. D. Allen and C. V. Senoff, *Chem. Commun.*, 621 (1965).
(156) A. D. Allen, *Advan. Chem. Ser.*, **No. 100**, 79 (1971).
(157) A. D. Allen, R. O. Harris, B. R. Loescher, J. R. Stevens, and R. N. Whiteley, *Chem. Rev.*, **73**, 11 (1973).
(158) J. K. Burdett, M. A. Graham, and J. J. Turner, *J. Chem. Soc. D*, 1620 (1972).
(159) H. Huber, E. P. Kündig, M. Moskovits, and G. A. Ozin, *J. Amer. Chem. Soc.*, **95**, 332 (1973).

plexes between metal atoms and N_2 in matrix isolation experiments. Of particular interest is the observation of a complex between Fe and N_2.[160] A band at 2020 cm^{-1} in the infrared spectrum of the matrix is assigned to the normal mode consisting mainly of N≡N stretch in the FeN_2 species. This is to be compared with a frequency of 2330 cm^{-1} for N_2 itself. The large shift to lower frequency is evidence of a considerable interaction between N_2 and Fe atoms.

The reaction of metal atoms with O_2 and N_2 under the low temperature conditions which obtain in the ionosphere are not expected to result in rupture of the diatomic molecule bond. Indeed, this would be a highly endothermic process for N_2 interaction with any of the metals of interest. The reaction

$$M + O_2 \rightarrow MO + O$$

is endothermic for Na and Mg and is probably just marginally exothermic for Fe. Unfortunately, the FeO dissociation energy is not well known; current best estimates[161,162] are 4.3 ± 0.5 eV.

Nothing is known of gas-phase species of the formula MO_2 for these three metals, but it seems highly unlikely that reaction of an atomic metal with O_2 at low temperatures which obtain in the mesosphere would result in rupture of the O-O bond, even if the process did lead to a gas-phase substance more stable than the metal atom–dioxygen complex. It seems extremely unlikely that the process would, in fact, be exothermic for Na or Mg; it may not be exothermic even for Fe. There are no reports in the modern literature of an FeO_2 gas-phase species. We therefore assume that the interaction of a metal atom with O_2 or N_2 leads to a complex of the metal atom with the intact O_2 or N_2 molecule. Just such an interaction between Ni and O_2 has been reported by Huber and Ozin[162a] on the basis of matrix isolation studies.

While the Fe–N_2 interaction is presumably linear, the metal–O_2 complexes probably involve a geometrical arrangement of the form

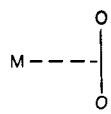

Metal complexes which have this geometry, as evidenced by thorough vibrational analysis or by X-ray structural characterization, are numerous.[153,163,164] The Co, Rh, Ir triad are particularly prone to forming O_2 complexes. Although the stabilities of the complexes vary greatly from metal to metal, with metal oxidation state, and with changes in the ligands on the metal, it is of interest to note the stabilities of the O_2 adducts formed by a group of complexes in which the metal is in the (+1) oxidation state. In this case the metal is isoelectronic in terms of metal orbital configuration with Fe^0. Ibers and coworkers[163] find that the order of stability is Ir > Rh > Co for a given set of ligands about the metal. Furthermore, with a given metal, stability increases as the ligands around the metal become more electron releasing. These observations are interpreted to mean that the metal–O_2 adduct stability increases with a lowering in effective charge on the metal. This suggests that Fe^0 should be capable of forming a reasonably stable adduct with O_2.

In condensed media the metals form dinitrogen and dioxygen complexes which contain several other coordinated ligands around the metal. These other ligands do influence the effective charge on the metal and availability of certain of the metal orbitals for interaction with O_2 or N_2, but there is no reason to suppose that they are essential in these respects for formation of complexes with O_2 or N_2. Their *essential* role in condensed media is to prevent rapid decomposition of the complexes by filling up the coordination sphere around the metal. Since this is not an essential function in the gas phase at low pressure and in the absence of significant concentrations of competing base molecules, the simple transition metal MN_2 and MO_2 species should be stable toward collisionally activated dissociation for several of the transition metals, and in particular for Fe, which concerns us here. In an analogous way the cluster ions FeO_2^+ and FeN_2^+ should possess significant stability due to covalent bond interaction involving the metal 3d orbitals, over and above that to be expected on the basis of the electrostatic calculations alone.

It is of interest to note that the $FeNO^+$ cluster ion, which is isoelectronic with FeCO or FeN_2, should be a particularly stable species. It is not considered in the chemical scheme, since its chemical role in the ionosphere should be essentially identical with that for FeN_2^+ or FeO_2^+, and the level of NO is sufficiently low[69] so that its reactions with the metals are never significant in relation to competing processes.

IX. Calculated Distributions of Metallic Species

The interconversions between various metal species shown in Figure 12 are assumed to occur in the context of a steady-state atmosphere of both neutral and ionic species whose concentrations are assumed not to be significantly perturbed by the presence of the metals. Except for depletion of NO^+ and O_2^+ in the sporadic E layers,[70,116] this assumption is probably satisfactory.

Concentrations of the relevant atmospheric constituents were estimated for conditions corresponding to daytime and predawn. Concentrations of many of the minor constituents, which are of importance for our calculations, are very poorly known from experimental results. There is the further problem that the levels of many species are known to vary widely with season, time of day, and the presence of disturbing effects. Accordingly, we have attempted to define a set of idealized concentration profiles which are representative and consistent with what is known of the levels obtaining at the times data on the metal distributions have been obtained. It develops, fortunately, that many of the more interesting features of the metal chemistry are not seriously dependent on the details of assumptions made in establishing the profiles.

The profiles chosen for the ionic species are depicted in Figures 13 and 14. The e^- profiles display the essential feature of a sharp drop in electron level below about 100 km.[29,30] The A^- profile was chosen so that there would be a drop in total negative charge concentration from 100 to 80 km, a 10-km region of constant level, and finally an order of magnitude drop in the range from 70 to 50 km. Since very little is known of the levels of ionization in this region, the profile below 70 km is rather arbitrary, but it is of no consequence for the metal ion distribution. The major feature of importance for the metal ion chemistry is the steep drop in electron level below 100

(160) (a) J. K. Burdett and J. J. Turner, private communication; (b) G. A. Ozin and A. Vander Voet, *Accounts Chem. Res.*, **6**, 313 (1973).

(161) "JANAF Thermochemical Tables," 2nd ed, National Bureau of Standards Reference Data System, NSRDS-NBS 37, Washington, D. C., 1971.

(162) A. G. Gaydon, "Dissociation Energies," 3rd ed, Chapman and Hall, Ltd., London, 1968.

(162a) H. Huber and G. A. Ozin, *Can. J. Chem.*, **50**, 3746 (1972).

(163) J. A. McGinnety, N. C. Payne, and J. A. Ibers, *J. Amer. Chem. Soc.*, 91, 6031 (1969).

(164) R. Mason, *Nature (London)*, **217**, 543 (1968).

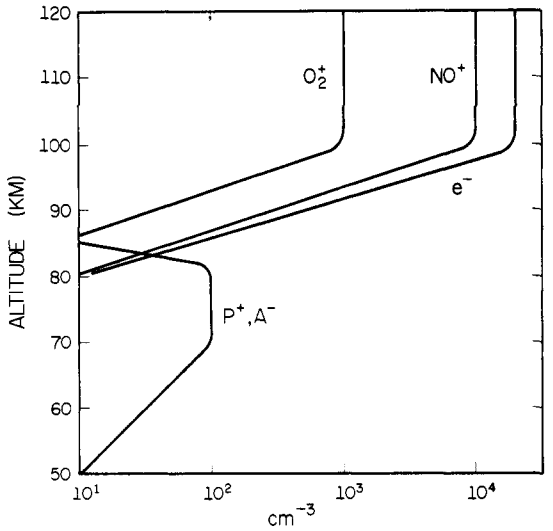

Figure 13. Assumed nighttime profiles of ionic species employed in calculations.

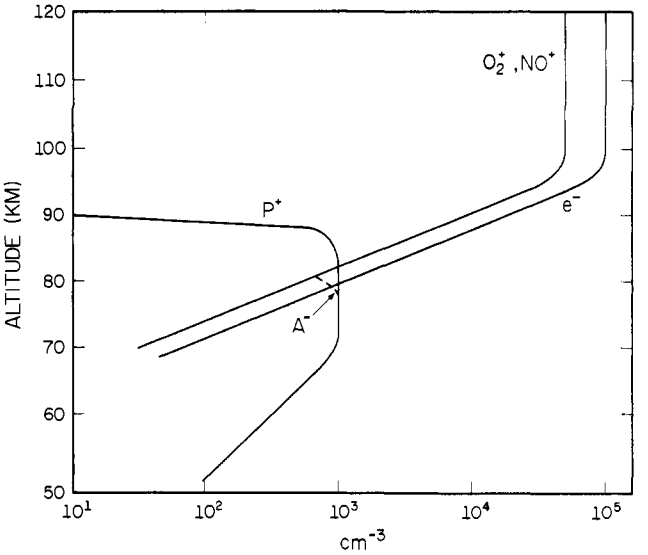

Figure 14. Assumed daytime profiles of ionic species employed in calculations.

km and the corresponding rapid increase in importance of negative ions below 85 km, features which correspond closely to observed electron and negative ion profiles.

The NO^+ and O_2^+ profiles assumed match quite well the observed profiles for these ions, although there is in fact great variability in the observations. The NO^+/O_2^+ ratios of 10 in nighttime and 1 in daytime are in accord with many reports,[165,166] but Aikin and Goldberg[103] report wide variations in the ratio in the equatorial E region. The growth of the cluster ions, particularly the hydronium hydrates, represented here by P^+, in the range of about 85 km is in accord with numerous positive ion mass spectral studies of this region.

The details of assumptions regarding the ion profiles in the region below about 90 km are of little importance for the metallic element chemistry, because the metals are predominantly in the form of neutral species below 90 km for any reasonable assumptions whatever about the profiles of the ionic species.

The assumed profiles for O_3 and O are shown in Figure 15. The daytime profile for O is in reasonable agreement with the profiles calculated by Crutzen[72,73] and Hunt,[74] and given by the COSPAR 1965 reference atmosphere.[2] The steep drop in the O level at night below 85 km is found in all models of the neutral atmosphere. The O_3 daytime profile corresponds roughly to the profiles given by both Crutzen and Hunt. The nighttime profile differs from the evening twilight profile in approximately the manner shown by Hunt.

The $O_2(^1\Delta_g)$ daytime profile is taken to be that given by Wood[71] for a solar elevation of 18°. The nighttime profile is much reduced from that. We have assumed the values given by Bishop, Baker, and Han.[167] These values are upper limits for undisturbed conditions, since they were obtained in weak auroral displays. The number densities of N_2 and O_2 were taken from the COSPAR 1965 reference atmosphere.

Other neutral atmospheric constituents which might be expected to undergo reactions with metallic species, *e.g.*, H, O_2H, H_2O, and NO, have been omitted from consideration, because the chemistry is completely dominated by other species present in relatively much higher concentrations, in particular O and O_3.

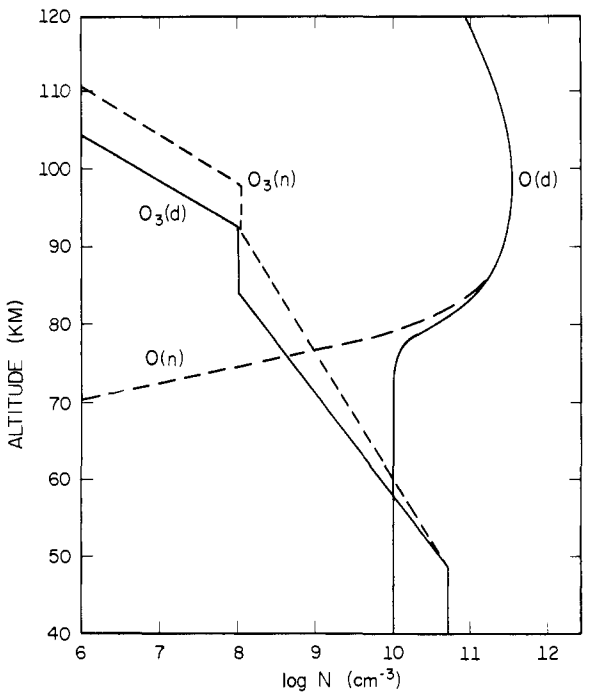

Figure 15. Assumed profiles for O and O_3. The label (n) refers to predawn conditions, (d) to daytime conditions.

Rate constants for the chemical processes shown in Figure 12 are given in Table X for sodium, magnesium, and iron. Where noted in the footnotes, rate constants were estimated for an assumed temperature of about 200°, since this is roughly representative of the temperatures in the region of the mesopause. In many instances values measured at about 300° were used without change. The temperature dependences of most of the reactions are not in any case likely to introduce uncertainties which are large in comparison with uncertainties in many of the rate constants themselves.

While values are available for rate constants for many of the reactions listed in Table X, no data are available for an even larger number. In such cases it was necessary to guess at a value, by analogy with the known rate constants for reactions which are as closely similar as possible. The bases for estimates made in this fashion

(165) R. S. Narcisi, A. D. Bailey, L. E. Wlodyka, and C. R. Philbrick, *J. Atmos. Terr. Phys.*, **34**, 647 (1972).

(166) T. J. Keneshea, R. S. Narcisi, and W. Swider, Jr., *J. Geophys. Res.*, **75**, 845 (1970).

(167) R. H. Bishop, K. D. Baker, and R. Y. Han, *J. Atmos. Terr. Phys.*, **34**, 1477 (1972).

TABLE X. Rate Constants for Reactions of Metallic Species

	Reaction	Na		Mg		Fe	
		Rate constant	Ref	Rate constant	Ref	Rate constant	Ref
1.	$M + O_2^+ \rightarrow M^+ + O_2$	6.0(−10)	43	1.2(−9)	42	1.1(−9)	*a*
2.	$M + NO^+ \rightarrow M^+ + NO$	0.8(−10)	43	8.0(−10)	42	9.2(−10)	*a*
3.	$M + P^+ \rightarrow M^+ + P$	24(−10)	*b*	8.0(−10)	*c*	1.5(−9)	*d*
4.	$M + h\nu \rightarrow M^+ + e^-$	$J = 1.7(-5)$	*e*	$J = 4.0(-7)$	*e*	$J = 5.0(-7)$	*e*
5.	$M + O_2 + X \rightarrow MO_2 + X$	1.0(−32)	*f*	1.0(−32)	*g*	1.0(−32)	*g*
6.	$M + N_2 + X \rightarrow MN_2 + X$	0	*h*	0	*h*	1.0(−32)	*g*
7.	$M + O_3 \rightarrow MO + O_2$	1.0(−13)	*i*	1.0(−13)	*i*	1.0(−13)	*i*
8.	$M + O_2(^1\Delta g) \rightarrow MO + O$	0	*j*	0	*j*	1.0(−14)	*k*
9.	$M + O + X \rightarrow MO + X$	1.0(−33)	*i*	1.0(−32)	*i*	1.0(−32)	*i*
10.	$M + O_2^+ \rightarrow MO^+ + O$	1.0(−10)	*l*	3.4(−10)	*m*	1.0(−10)	*g*
11.	$M^+ + e^- \rightarrow M$	1.0(−12)	62	1.0(−12)	62	1.0(−12)	62
12.	$M^+ + A^- \rightarrow M + A$	1.0(−7)	*g*	1.0(−7)	*g*	1.0(−7)	*g*
13.	$M^+ + O_2 + X \rightarrow MO_2^+ + X$	5.0(−32)	*m, o*	5.0(−30)	54	2.5(−30)	54
14.	$M^+ + N_2 + X \rightarrow MN_2^+ + X$	1.0(−31)	*p*	1.0(−31)	*q*	2.5(−30)	*r*
15.	$M^+ + O + X \rightarrow MO^+ + X$	1.0(−30)	*q*	5.0(−30)	*q*	2.5(−30)	*r*
16.	$M^+ + O_3 \rightarrow MO^+ + O_2$	1.0(−12)	*s*	2.0(−10)	54	1.5(−10)	54
17.	$MO_2^+ + X \rightarrow M^+ + O_2$	1.0(−12)	*n, o*	1.0(−13)	*t*	1.0(−15)	*g*
18.	$MN_2^+ + X \rightarrow M^+ + N_2$	1.0(−13)	*n, o*	1.0(−14)	*t*	1.0(−15)	*g*
19.	$MO_2^+ + O \rightarrow MO^+ + O_2$	1.0(−10)	*g*	1.0(−10)	*g*	1.0(−10)	*g*
20.	$MN_2^+ + O \rightarrow MO^+ + N_2$	1.0(−10)	*g*	1.0(−10)	*g*	1.0(−10)	*g*
21.	$MN_2^+ + e^- \rightarrow M + N_2$	2.0(−6)	*g*	2.0(−6)	*g*	2.0(−6)	*g*
22.	$MO_2^+ + e^- \rightarrow M + O_2$	2.0(−6)	*g*	2.0(−6)	*g*	2.0(−6)	*g*
23.	$MO^+ + O \rightarrow M^+ + O_2$	1.0(−10)	*u*	1.0(−10)	54	1.0(−10)	*u*
24.	$MO^+ + e^- \rightarrow M + O_2$	4.0(−7)	*g*	4.0(−7)	*g*	4.0(−7)	*g*
25.	$MO^+ + e^- \rightarrow MO + h\nu$	0	*g*	0	*g*	0	*g*
26.	$MO^+ + A^- \rightarrow MO + A$	1.0(−7)	*g*	1.0(−7)	*g*	1.0(−7)	*g*
27.	$MO_2 + O \rightarrow MO + O_2$	1.0(−11)	*g*	1.0(−11)	*g*	1.0(−11)	*g*
28.	$MN_2 + O \rightarrow MO + N_2$	...		...		1.0(−11)	*g*
29.	$MO + O \rightarrow M + O_2$	1.0(−11)	*g*	1.0(−11)	*g*	1.0(−11)	*g*
30.	$MO + O_2^+ \rightarrow MO^+ + O_2$	5.0(−10)	*g*	8.0(−10)	*v*	8.0(−10)	*v*
31.	$MO + NO^+ \rightarrow MO^+ + NO$	5.0(−10)	*g*	8.0(−10)	*v*	8.0(−10)	*v*
32.	$MO + h\nu \rightarrow MO^+$	?	*w*	?	*w*	?	*w*
33.	$MO_2 + O_3 \rightarrow MO + 2O_2$	1.0(−14)	*g*	1.0(−14)	*g*	1.0(−15)	*g*
34.	$MN_2 + O_3 \rightarrow MO + N_2 + O_2$	...		...		1.0(−15)	*g*
35.	$MO + O_3 \rightarrow MO_2 + O_2$	0	*x*	1.0(−16)	*x*	1.0(−16)	*x*
36.	$MO + O_3 \rightarrow M + 2O_2$	1.0(−16)	*x*	0	*x*	0	*x*

[a] J. A. Rutherford and D. A. Vroom, *J. Chem. Phys.*, **57**, 3091 (1972). [b] J. A. Rutherford, R. F. Mathis, B. R. Turner, and D. A. Vroom, *ibid.*, **55**, 3785 (1971), give a value of 27×10^{10} cm^3 sec^{-1} for the rate constant of the reaction $Na + H_2O^+ \rightarrow Na^+ + H_2O$. The cross-section *vs.* energy curves are quite similar for H_2O^+ and H_3O^+ reactions with Na. The value listed for k_3 is, however, only a rough estimate. [c] Estimated. The reaction $Mg + H_3O^+ \rightarrow Mg^+ + H + H_2O$ is endothermic for ground-state reactants, but $Mg + H_3O^+ \rightarrow MgH^+ + H_2O$ is undoubtedly exothermic. Accurate rate constant data, however, are not available (see ref 43). [d] The process $Fe + H_3O^+ \rightarrow Fe^+ + H_2O + H$ is endothermic,[a] but $Fe + H_3O^+ \rightarrow FeH^+ + H_2O$ is exothermic. Rate is estimated to be equal to that for the charge-transfer reaction with H_2O^+. [e] The value given represents an estimated upper limit for the photoionization rate (section II.C). Photoionization has been neglected in the calculations, except where indicated in the text. [f] Estimated; F. Kaufman, *Can. J. Chem.*, **47**, 1917 (1969), discusses this reaction. [g] Estimated. [h] Should be of negligible importance; see text for discussion. [i] Estimated; see Table VIII. [j] Endothermic. [k] This reaction is probably just barely exothermic.[161,162] [l] Branching ratio between reactions 1 and 10 is on the order of 15–20%: P. K. Rol and E. A. Entemann, *J. Chem. Phys.*, **49**, 1430 (1968). Reaction 10 is exothermic by about 3.1 eV: D. L. Hildenbrand and E. Murad, *J. Chem. Phys.*, **53**, 3403 (1970). [m] P. K. Rol and K. L. Wendell, Research Report, Research Institute for Engineering Sciences, Wayne State University, Detroit, Mich., Final Report, Project No. 5710, 1971. [n] K. G. Spears, *J. Chem. Phys.*, **57**, 1850 (1972). [o] R. A. Beyer and G. E. Keller, *Trans. Amer. Geophys. Union*, **52**, 303 (1972). [p] Estimated. Set a factor of 2 larger than k_{13} because the NaN_2^+ binding is calculated[n] to be somewhat higher than for NaO_2^+. [q] Estimated; see ref 54. [r] No experimental data are available but should be about the same as for k_{13} on the grounds of comparable stability. [s] Estimated; see k_{16} for Mg^+. [t] Estimated; should be smaller than the analogous, known reaction rate for Na^+ because Mg^+ is more polarizable.[n] [u] Estimated; see k_{23} for Mg^+. [v] The values of k_{30} for Mg and Fe should be higher than for Na on the grounds of nearer approach to resonant charge transfer, but no data are available. The value for Fe could conceivably be much higher because of a higher density of excited states involving the 3d electron excitations in FeO^+. [w] At the altitudes at which MO is prevalent, direct photoionization should be of negligible importance. [x] Where reaction 35 is highly exothermic, we assume that reaction 36 predominates. Reaction 36 should be just slightly endothermic for FeO and only marginally exothermic for MgO. Accordingly, k_{36} is assumed to be zero in these cases.

are indicated in the individual footnotes. It is perhaps worthwhile, however, to make a few general comments. No account has been taken of spin multiplicity changes in estimating reaction rates. Aside from the fact that the spin states of many of the metal-containing species are uncertain, there is little evidence that the Wigner spin conservation rule is of importance in determining the rate constants. Further, in the case of Fe, spin–orbit coupling is doubtless sufficiently large to invalidate the rule.

In cases where considerable uncertainty exists in the estimated values, a value in the middle of the range of plausible values has been chosen. In addition, calculations were carried out in which some of the more critical but experimentally unknown rate constants were varied

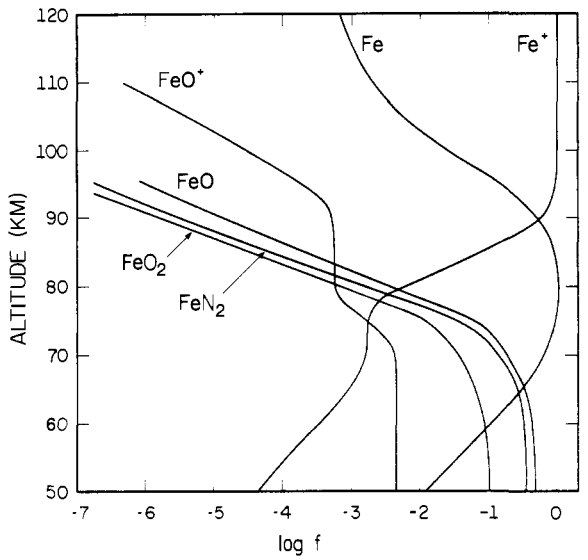

Figure 16. Calculated daytime distribution of iron species. The fractional abundance of each species is symbolized by f.

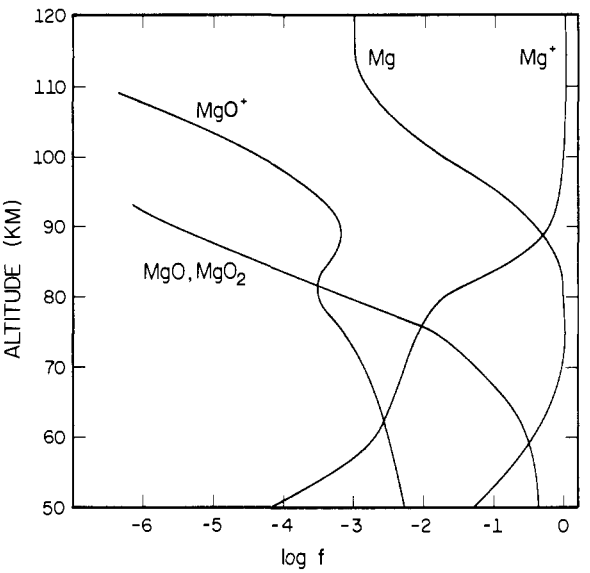

Figure 18. Calculated daytime distribution of magnesium species.

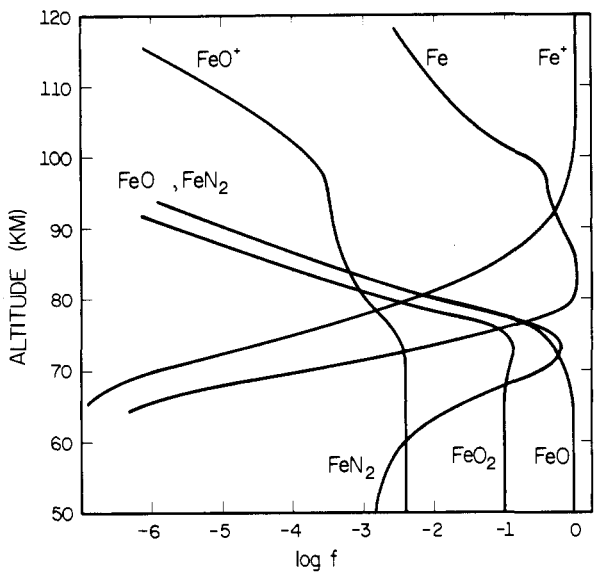

Figure 17. Calculated nighttime distribution of iron species.

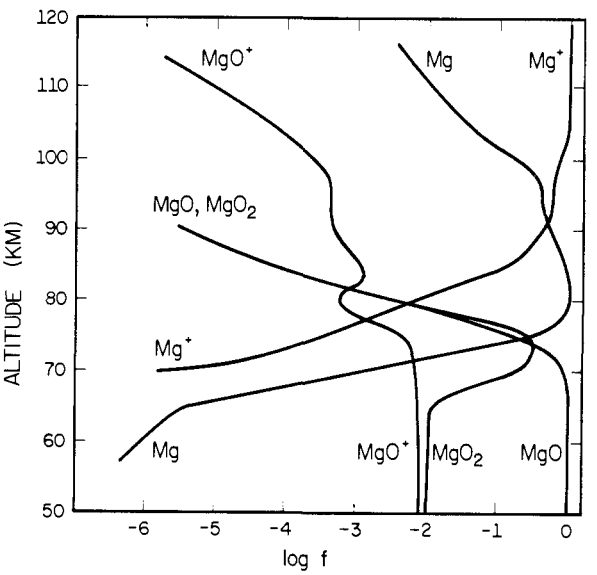

Figure 19. Calculated nighttime distribution of magnesium species.

over wide limits to determine the sensitivity of the results to the assumptions made.

The calculations were performed by setting the complete time dependence expression for each metallic species to zero, inserting the appropriate rate constants and concentrations for each of the atmospheric constituents, and solving the resultant set of simultaneous equations for the relative concentrations of the metal species (*i.e.*, by arbitrarily setting (M) = 1). The calculations were carried out for constituent concentrations corresponding to closely spaced intervals of altitude in the range 50–120 km, and for both day and night conditions. For each set of concentrations the calculations were repeated for a 10% change in each rate constant and concentration, in turn, to determine the sensitivity of the calculated metal species concentrations to the uncertainties in the input parameters.

The derived metal species profiles, expressed as log (fractional relative abundances), are depicted for Na, Mg, and Fe under both day and night conditions, in Figures 16–21. The profiles for MO_2^+ and MN_2^+ are omitted from the figures since these species do not have an appreciable abundance at any altitude.

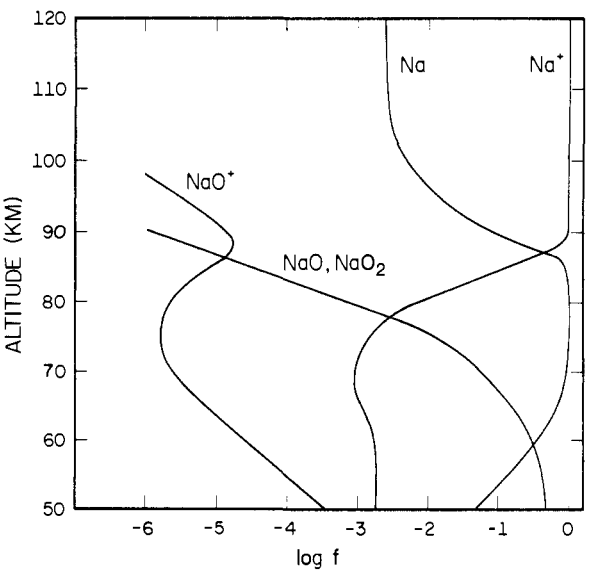

Figure 20. Calculated daytime distribution of sodium species.

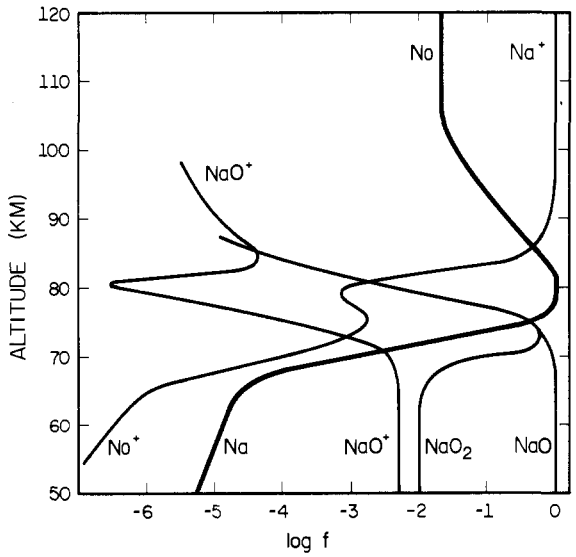

Figure 21. Calculated nighttime distribution of sodium species.

An additional quantity derived from the calculations, the weighted average lifetime of the positively charged species, τ, is graphed for iron in Figure 22. This quantity is defined as

$$\frac{1}{\tau_+} = \{[e^-]\sum_i (M_i^+)k_{ei} + [A^-]\sum_i (M_i^+)k_{Ai}\}/\sum_i (M_i^+) \quad (26)$$

where (M_i^+) represents one of the four charged species, and k_{ei} and k_{Ai} represent the rate constants for recombination with electrons and neutralization with negative ions, respectively. It is of interest in assessing the time scale on which chemical processes lead to a change in charge state, as compared with the time scales on which diffusion and layering occur.

The calculated results provide a model for the distribution of each of the three metals among the various possible chemical species considered, assuming that transport and diffusion processes are absent. Since they depict a *relative* distribution, no assumption is made about the mixing ratio of each metal *in toto* as a function of altitude. Before proceeding to a more detailed consideration of some of the results, it is appropriate to consider whether the chemical processes considered can be reasonably expected to dominate in determining the relative concentrations of the species involved, and at what altitudes and under what conditions this can be expected to hold.

It is clear from the profiles shown that, above about 90 km, the major metallic species present is the free metal ion. Accordingly, the time scale on which chemical change occurs above this altitude is essentially the value of τ_+, since this quantity represents the average lifetime of M^+, regardless of whether M^+ undergoes radiative recombination or is neutralized *via* one of the other charged species. As Figure 22 shows, the calculated lifetime for the positive species above about 90 km is much longer than 24 hr. The characteristic time constant for diffusion, τ_D, is given by $\tau = H^2/D$, where H is the scale height and D is the eddy diffusion constant. For $D = 4 \times 10^6$ cm^2 sec^{-1} and a scale height of about 4 km, τ_D is on the order of 24 hr. This means that transport mechanisms such as layering due to wind shears, and eddy diffusion, should play an important role in determining the distribution of the ions.

The average lifetime of the neutral metal atom, τ_M, in the altitude range 90 km and upward is given by $1/[k_1(O_2^+) + k_2(NO^+)]$. It is of interest to know how this time compares with characteristic eddy diffusion time constants. During daytime τ_M at 100 km and above for Na, Mg, and Fe is about 3×10^4, 1×10^4, and 1×10^4 sec, respectively, neglecting any contribution from photodissociation. During nighttime the average lifetimes are longer because of the lower concentrations of NO^+ and O_2^+. The much lower concentration of O_2^+ is of special importance in the case of Na, since k_2 for Na is smaller by an order of magnitude than k_1 (Table X).

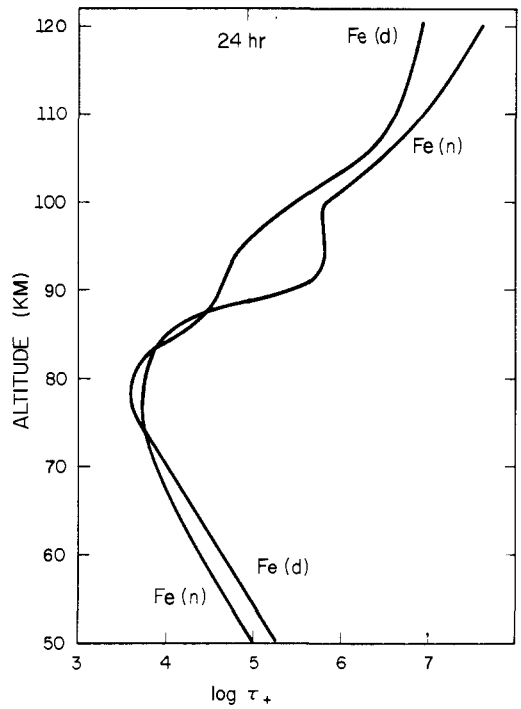

Figure 22. Variation in τ_+ for the iron system as a function of altitude for both daytime (d) and nighttime (n) conditions. The curves for Na and Mg are closely similar.

It appears, therefore, that the neutral metal atoms produced by meteor ablation are oxidized to M^+ on a time scale of several hours. For an eddy diffusion coefficient $\sim 4 \times 10^6$ cm^2 sec^{-1}, the root-mean-square displacements of the metal atoms in this time interval are on the order of several kilometers. The particular significance of these considerations for the sodium atom layer is discussed below.

A. Iron

Calculated daytime and nighttime distributions for iron are depicted in Figures 16 and 17. It is noteworthy that the crossover point in the Fe/Fe^+ ratio is very little different in the two cases. Furthermore, the scale height for Fe^+ on the lower side is comparable in the two cases, about 1.2–1.4 km. As is the case for all the metals, the singly charged atomic ion is the only charged species with significant abundance throughout the altitude range. It is of interest, however, that the model predicts a 10^{-3} relative abundance for FeO^+ to above 90 km, the altitude region in which Narcisi reports a weak FeO^+ signal.[168]

The opportunities for comparisons of the calculated quantities with observational data are quite limited. The observations of Fe^+ at altitudes above 90 km are certainly consistent with the model. The average lifetime of Fe^+ above 90 km is more than long enough for wind shear effects to cause layering when the wind structure is appropriate. The lifetime of the positive ions is suffi-

(168) R. S. Narcisi in "Physics and Chemistry of Upper Atmospheres," B. M. McCormac, Ed., D. Reidel Publishing Co., Dordrecht, Holland, 1973, p 73.

ciently short below about 86 km, however, to ensure that the level of Fe^+ should not be significant as a result of either the downward sweeping action of the wind shear or diffusion.

The only published experimental chemistry of iron in the ionosphere was reported recently by Rosenberg and coworkers.[169] They streamed several kilograms of $Fe(CO)_5$ from a rocket in the altitude intervals 88–125 and 129–145 km, during twilight. Emission from FeO was seen *via* a ground-based spectrograph. The FeO emissions came up very quickly and persisted for up to only 3 sec. Presumably $Fe(CO)_5$ is rapidly converted by atomic oxygen to FeO, which is then removed by further reaction with O to produce Fe.

If the process $FeO + O \rightarrow Fe + O_2$ is to have a half-life of, say, 1 sec, then $k_{29}(O)$ is on the order of about 0.6 sec^{-1}. Assuming $(O) = 1 \times 10^{11}$ cm^{-3}, k_{29} is on the order of 7×10^{-12} cm^3 sec^{-1}. Considering the crudity of the estimates involved, this is in reasonable agreement with the assumed value of 10×10^{-12} (Table X).

Below 90 km the most striking difference in the day and nighttime distributions is in the Fe profile. In daytime, when the O level is high, Fe is the dominant chemical species to well below 70 km. Photoionization of Fe, ignored in the calculation, cannot significantly deplete the Fe level. On the other hand, photodissociation of the neutral molecular species, FeO, FeO_2, and FeN_2, could very well make the Fe level higher than shown, even in the 60-km region.

In marked contrast the Fe concentration at night falls off with a scale height of only 0.6 km, reflecting the sharp drop in the assumed O concentration. This particular feature is relatively insensitive to the assumptions made about various rate constants involving the neutral species. Figure 23 shows the profiles of iron species at night, assuming $k_4 = k_5 = 3.0 \times 10^{-31}$ cm^6 sec^{-1}, and $k_{32} = k_{33} = k_{34} = 0$. The effect of a 30-fold increase in the rates of the three-body reactions is to raise the lower boundary of the Fe profile by about 2 km.

The values assumed for k_{32}, k_{33}, and k_{34} affect the calculated *equilibrium* distributions of the neutral molecules. It is important, however, to consider the time constants involved. In the chemical loop involving the neutral species

$$Fe \xrightarrow{1} FeO_2, FeN_2 \xrightarrow{2} FeO \xrightarrow{3} Fe$$

the conversion of Fe to FeO_2 or FeN_2 is fast at all altitudes below about 80 km. As the atomic oxygen level decreases after sunset, however, conversions 2 and 3 become determined by the rate constants for the O_3 reactions. The values given in Table X are probably upper limits. Reactions 2 and 3 could in fact be so slow that the effective half-lives are on the order of days. In this case, the relative concentrations of FeO, FeO_2, and FeN_2 shown in Figures 17 and 23 are of no significance. The Fe levels established during daytime, when all stages of the cycle are relatively fast, would then be converted essentially entirely into FeO_2 and FeN_2. There is thus good reason to expect that FeO_2 and FeN_2 should be important and perhaps the dominant iron species in the night sky in the altitude range from 80 to 50 km. The relative concentrations of FeO, FeO_2, and FeN_2 cannot be predicted at present. The relative rates of the important reactions involving the neutral species are not known. A switching reaction of the form

(169) G. T. Best, C. A. Forsberg, D. Golomb, N. W. Rosenberg, and W. K. Vickery, *J. Geophys. Res.*, 77, 1677 (1972).

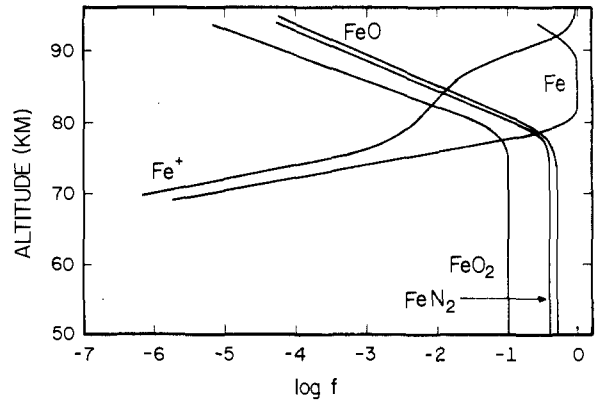

Figure 23. Calculated distribution of iron species at night, assuming $k_4 = k_5 = 3.0 \times 10^{-31}$ cm^6 sec^{-1} and $k_{32} = k_{33} = k_{34} = 0$.

$$FeO_2 + N_2 \rightarrow FeN_2 + O_2$$

or its reverse if FeO_2 is the more stable species, should be facile. Thus, one of the two species will probably be found to predominate. We speculate that FeN_2 will prove the more stable. The formation of adducts of the metals with more than one O_2 or N_2 molecule may provide a complicating feature in the chemistry of the neutral metal atoms in the atmosphere.[160] Thus, for example, processes of the form $X + FeN_2 + N_2 \rightarrow Fe(N_2)_2 + X$ or $X + FeN_2 + O_2 \rightarrow Fe(N_2)(O_2) + X$ might occur. The possibilities of these and similar reactions involving still higher coordination numbers about the metal are real, but in the absence of kinetic and equilibrium data it seems inadvisable to extend the speculative discussion beyond consideration of the simplest systems.

There is a need for experimental studies of the kinetics of formation and reactions of the neutral iron molecular species. Before experiments could be designed which might reveal their presences and distributions in the mesosphere, it will be necessary to observe their physical properties in laboratory-based experiments. Although the experimental challenges are formidable, it would appear from the model presented here that the simple neutral compounds are deserving of investigation.

B. Magnesium

The principal features of the magnesium system at 110 km, particularly as regards the relative abundances of Mg and Mg^+, have been considered by Anderson and Barth.[90] The results presented in Figures 18 and 19 do not reveal any significant points of difference.

The results for the profiles of the Mg species are similar in most respects to those seen for iron. As in the case of iron, the relative abundances of the neutral species below about 80 km during nighttime cannot be predicted at present for lack of information about the relevant rate constants. We have assumed that MgN_2 does not possess sufficient stability to persist in significant concentration, so the competing neutral species are MgO and MgO_2.

It is noteworthy that in the altitude range 90–100 km the MgO^+ level is 1×10^{-3} or less that of Mg^+. Since Ca in chondrites is about 0.05 as abundant as Mg, it seems quite unlikely that the mass 40 ion seen in the mass spectral studies could be MgO^+, if the metals are meteoric in origin.

C. Sodium

The calculated distributions for sodium species are shown in Figures 20 and 21 for day and nighttime condi-

tions, respectively. The nighttime distribution is of particular interest, since it may be compared with the extensive and reliable data on the sodium atom layer.

The calculations show a cross-over from Na^+ to Na as the predominant species in the vicinity of 86 km at night and 87 km during day, in reasonable agreement with the experimental observations of a maximum in the sodium atom layer in the range 88–92 km, depending on season, and observations of a Na^+ maximum in the vicinity of 90–95 km.

The model predicts an Na^+/Na nighttime ratio greater than 1 at 90 km, whereas the observations suggest a ratio on the order of 10^{-2} to 10^{-1}. The discrepancy could be accounted for in terms of altered profiles for NO^+ and O_2^+, but it is equally true that the temporal nature of the source for sodium, and transport processes, could be responsible. The limitations of the model presented here should again be recalled. No assumption is made regarding the number density profile of each metal *in toto* as a function of altitude. This will be a function of the altitude profile characteristics of the source, the transport characteristics of the atmosphere with respect to both neutral and charged components, as well as of the chemistry. Thus, the chemical model does *not* predict that the nighttime maximum in the sodium level should be at 80 km (Figure 21). Rather, it says that the abundance of atomic sodium relative to other forms of the element should be greatest at this elevation, *assuming that steady-state equilibria are attained.*

Sodium ion is the predominant species at all altitudes above the cross-over altitude. The calculated values of τ_+ for nighttime conditions extend from 1.0×10^5 sec at 70–80 km to about 5×10^7 sec at 110 km and above. The lifetime of Na with respect to oxidation to Na^+ is about 7×10^5 sec at 100 km for nighttime conditions but much shorter in the day, about 3×10^4 sec. This particular point is of interest in connection with the question of whether the sodium seen in the sodium layer arises directly from sodium atoms ablated from meteoroids or whether, on the other hand, the sodium atoms so produced undergo ionization, transport to lower altitudes, and subsequent reduction to atomic sodium at about 90 km. The observations of an increase in the entire envelope of the sodium layer during the night hours at the peak time of a Geminids meteor shower[93] would suggest that some, at least of the sodium seen in the layer, is freshly deposited. This is consistent with Gadsden's model, which predicts a maximum ablation rate per unit of altitude in the vicinity of 90 km.

As indicated in section VII, the average rate of metal atom deposition from meteoroid ablation is estimated to be on the order of 10^6 metal atoms cm^{-2} sec^{-1}. Assuming that about 1% of these are sodium, and assuming an observational period of a few hours, *i.e.*, about 10^4 sec, additional sodium added to the layer would at maximum (*i.e.*, assuming that all the ablated material appeared in the layer) amount to about 10^8 atoms cm^{-2}, distributed over a height interval of perhaps 10 km. Thus, during more or less normal conditions of meteoroid activity, there should be no observable growth in the sodium layer at night as a result of heavier meteor activity during the night hours. During periods of especially heavy meteor activity, however, a several-fold increase might easily be observed.

Gibson and Sandford have reported[92] observation of an Na layer at about 103 km on two occasions in the course of their nighttime laser ranging studies. They suggest that the sodium atoms might have been produced *via* reduction of Na^+ layered at this elevation. But Na cannot achieve a concentration by this means higher than the equilibrium concentration of Na as predicted by the model, since the time constant for oxidation of Na is shorter than for reduction of Na^+. The calculated ratio Na^+/Na at 103 km is on the order of 100 for both day and night conditions. If the level of Na^+ in the metal ion layer were as high as 10^3 cm^{-3} (consistent with maximum levels of about 10^5 cm^{-3} observed for Fe^+ and Mg^+), the Na level could at most be about 10 cm^{-3}. This is about an order of magnitude too small to give rise to the observations. It seems probable, therefore, that Na layers seen at elevations above 100 km are due to a primary source of the neutral atoms, *e.g.*, meteoroid influx.

One of the most interesting features of the calculated nighttime distribution for sodium is the extremely small scale height of about 0.6 km for the lower boundary of the sodium layer. This sharp boundary is the result of the assumed profile for atomic oxygen, and it is to be expected that its development would be linked to the development of the atomic oxygen profile in the early hours of the night. It is interesting that just such a sharp lower boundary has been observed[93] in laser radar studies of the sodium layer throughout the early night hours. Hake and coworkers[93] appear to have rejected atomic oxygen variation as the source of the sharp profile for Na. The alternatives suggested by these authors, however, such as interactions with the water cluster ions which maximize at 80–85 km, must be ruled out on the grounds that the number densities are inadequate to provide an acceptable removal mechanism. The total water cluster ion density does not exceed 10^4 cm^{-3} during the day and decreases after sunset. It would require an exceptionally high charge-transfer rate constant for these reactions to be of importance in affecting the sodium layer, to say nothing of the fact that the diurnal variation is in the wrong direction.

The calculated profile for atomic sodium in the daytime shows a very broad maximum, extending to rather low altitude. This particular feature is not in agreement with the limited observational data available. The daytime measurements using laser ranging[107] do not possess a large working range in the Na level, so do not give an accurate description of the lower boundaries of the layer, below a factor of perhaps 10 from the maximum. The only other reported measurement of the sodium layer profile in daytime is the rocket-borne airglow photometer experiment reported by Donahue and Meier.[89] These authors give no indication of the range of sodium level covered by the measurements, but indicate only that the layer was observed to decrease exponentially from the maximum with a scale height of only 2.4 km.

It is possible to account for the observations by assuming that the sodium ion and sodium atom layers in the vicinity of 90 km represent bulges in the total sodium profile, as a result of source and transport processes. Sodium ions formed above 90 km by oxidation of sodium atoms are swept downward by the secular component of the ionospheric winds, to contribute to the maximum in the sodium ion profile at about 90–95 km, a maximum which may be assumed to be more or less coincident with the more obvious Fe^+ and Mg^+ maxima. Reduction of Na^+ adds to the sodium atom layer, which is probably due mainly to meteoroid ablation in the vicinity of 90 km. Sodium and the other metals find their way to lower elevations *via* diffusion. The sink for the metals (in the sense that they no longer persist as small, gas-phase molecules) is unknown but may be assumed to lie below 50 km. A relatively shallow concentration gradient of perhaps a factor of 10 over the altitude range 85–70 km would, however, probably be sufficient to preclude observation of atomic sodium much below the maximum in the

daytime Na profile with the experimental techniques employed to date. Anticipated improvements in laser ranging equipment should make it possible in the near future to more completely determine the nature of the lower side of the profile in the daytime. The prediction based on the model presented here is that the scale height will be large, on the order of perhaps 10 km, following an initial sharper drop of perhaps a factor of 10 from the maximum.

The effects of solar radiation were examined by carrying out the calculation for the sodium system using the daytime parameters and assuming that the ionization rate given in Table X for unattenuated solar radiation applies over the entire altitude range for both Na and NaO. The effect is, of course, to increase the Na^+ and NaO^+ levels at the expense of Na and NaO, respectively. The crossover point in the Na^+/Na distributions occurs at 85 km, as compared with 87 km when photoionization is neglected. The minimum value of log f for Na^+ with photoionization is -1.0 at about 72 km. Use of the ionization rate calculated from unattenuated solar radiation over the entire altitude range may lead to a slight overestimation of the ionized species, but the errors so incurred are small relative to several other uncertainties. Photodissociation of NaO and NaO_2 might also be expected to occur. The most one can say at present, therefore, is that the direct influence of solar radiation on the sodium system should be to shift the equilibria materially in the direction of the ionized or dissociated species.

D. General Remarks

The emphasis in the foregoing has been on the three most abundant metals in the ionosphere, iron, sodium, and magnesium. Both chromium and nickel closely parallel iron in chemical behavior as regards the chemical system shown in Figure 10 and may be expected to display closely comparable distribution profiles. Aluminum should be roughly comparable with Mg.

The chemistry of silicon is more complicated than for the metals; several pieces of thermochemical information necessary to a proper understanding of its ionospheric chemistry are missing. Swider[22,147] has suggested that the relative absence of Si^+ in the metal ion layer at 90–95 km may be due to the fact that the reaction $SiO_2^+ + O \rightarrow SiO^+ + O_2$ is endothermic. This could be the case if the SiO_2^+ is the conjugate ion of the SiO_2 molecule in which there are two strong Si–O bonds. If, however, the three-body reaction of Si^+ and O_2 at the relatively low temperatures of the ionosphere leads to a metastable complex between Si^+ and the O_2 molecule, as postulated above for the metals, reaction with atomic oxygen should be highly exothermic. The form in which silicon appears upon ablation from meteoroids is not known. The thermochemical work of Hildenbrand and Murad[170] and the kinetic study by Fehsenfeld[171] are in agreement in concluding that the reaction

$$SiO^+ + O \rightarrow Si^+ + O_2$$

should be exothermic. Fehsenfeld reports a rate constant of 2×10^{-10} cm^3 sec^{-1}. This means, conversely, that the reaction $Si^+ + O_2 \rightarrow SiO^+ + O$ is endothermic. In light of these considerations it is not clear why Si^+ and SiO^+ are seen in the higher metal ion layer but not in the lower.

Swider[22,147] has considered the chemistry of the metallic elements in considerable detail. He raises the possibility of several reactions which have not been included in the reaction scheme in Figure 12 and Table X. Radiative association of M^+ with O, $M^+ + O \rightarrow MO^+ + h\nu$, would provide an additional pathway for reduction of M^+ in the altitude region where M^+ is the predominant ion and three-body reaction rates are low, *i.e.*, above perhaps 100 km. The rate of the radiative association reaction is not known, but such reactions are very slow.

The ultimate fate of the metal ions is difficult to predict. Over a long period of time, clustering reactions may be expected to occur.

$$M + M + X \rightarrow M_2 + X$$

$$M_2 + M + X \rightarrow M_3 + X, \text{ etc.}$$

The low number density of the metals ensures, however, that such reactions will be slow. Furthermore, they will be essentially reversed by exothermic reactions of the form

$$M_2 + O \rightarrow MO + M$$

$$M_2 + O_3 \rightarrow MO + O_2 + M$$

It is difficult to visualize chemically plausible aggregation reactions which are not readily undone by O or O_3. The metals probably remain in the form of small atoms and molecules to at least an altitude of 50 km.

By way of summary, it would appear that the observations of the metallic elements in the lower ionosphere and upper mesosphere can be fairly well accounted for in terms of the chemical processes embodied in Figure 12. At the same time, a detailed accounting of the diurnal variations can be accomplished only by taking explicit account of the time dependence of the relevant ionic and neutral atmospheric minor constituents, as well as photoionization and photodissociation. In addition, some accounting must be taken of transport, in the form of eddy mixing, and both vertical and horizontal winds. An attempt has been made to do this, particularly for the ionic species.[70,172]

Acknowledgments. I am grateful to those who have graciously supplied me with requested figures, reprints, and preprints. The review was begun during a sabbatical leave stay as visiting scientist at the International Meteorological Institute in Stockholm. I am particularly grateful to Bert Bolin, Director, and to Georg Witt for their hospitality and many assistances. This work was supported in part by the National Science Foundation through Research Contract GH-33634 and Research Grant GP-30256X.

(170) D. L. Hildenbrand and E. Murad, *J. Chem. Phys.*, **51**, 807 (1969).
(171) F. C. Fehsenfeld, *Can. J. Chem.*, **47**, 1808 (1969).
(172) M. A. MacLeod, T. J. Keneshea, and R. S. Narcisi, *EOS, Trans. Amer. Geophys. Union*, **53**, 464 (1972).